TRACE ELEMENT DISTRIBUTION AND ALTERATION STUDY OF THE COPPER CITIES DEPOSIT, ARIZONA

By

THOMAS WILLIS REED

Bachelor of Science

Oklahoma State University

Stillwater, Oklahoma

1973

Submitted to the Faculty of the Graduate College
of the Oklahoma State University
in partial fulfillment of the requirements
for the Degree of
MASTER OF SCIENCE
July, 1975

TRACE ELEMENT DISTRIBUTION AND ALTERATION

STUDY OF THE COPPER CITIES

DEPOSIT, ARIZONA

Thesis Approved:

Zuhair al-Shaieb
Thesis Advisor

John Trammell

John C. Stone

N N Durham
Dean of the Graduate College

PREFACE

The Copper Cities deposit, like other porphyry copper deposits in Arizona, was discovered and exploited because of its surficial exposure. Geochemical exploration methods did not play a major role in the discovery of the deposit. The search for future, hidden deposits, such as those under pedisediments in the southwestern United States, will by necessity employ geochemical methods for exploration techniques. It is the aim of this study to add new information to the geochemical knowledge of porphyry copper systems and to aid future exploration methods.

The writer wishes to express his gratitude to Dr. Zuhair Al-Shaieb, thesis advisor, for his guidance and interest in the thesis project, and for his aid in the analytical procedures. Special thanks are also due Dr. John W. Trammell, Dr. John E. Stone, and Dr. John W. Shelton for their critical evaluations and helpful hints during the course of the study. The author is indebted to Mr. R. W. Hughes and Mr. Joseph E. Fowells of the Miami Copper Operations of Cities Service Minerals Corporation for their cooperation and assistance during the completion of the field work for this project. The use of company data and drill cores, and access to the mining operations is greatly appreciated. The writer is also grateful to the staff of Cities Service Minerals Corporation, in Tucson and Salt Lake City, for their helpful consultations and for the gracious loan of gold and silver element lamps for atomic absorption spectrophotometry analysis.

TABLE OF CONTENTS

Chapter Page

LIST OF TABLES

LIST OF FIGURES

Figure Page

CHAPTER I

ABSTRACT

The Copper Cities porphyry copper deposit is located near the town of Miami, Arizona. Mineralization is associated with the Late Cretaceous Lost Gulch quartz monzonite porphyry. The predominant hypogene sulfides are pyrite and chalcopyrite, and the supergene sulfides are chalcocite and covellite. Samples were collected from mine benches and drill cores and were analyzed for clay minerals and trace element content. The average copper and molybdenum grade are .35 and .0065 percent respectively.

Four hydrothermal alteration zones are present in the deposit. The potassic zone, containing secondary K-feldspar and biotite, forms a deep core below the ore body. The phyllic zone, characterized by maximum sericitic alteration, occurs above the potassic core in a central zone containing the ore body. The third zone, intermediate argillic alteration, is represented by calcium montmorillonite and kaolinite. This alteration is located on the fringes of the phyllic zone. The propylitic zone is the limit of significant hydrothermal alteration on the borders of the deposit.

A supergene kaolinite "blanket" was identified in the ore body beneath the base of the secondary chalcocite zone. The kaolinite "blanket" reflects the orientation of the local ground-water table. It formed from sericite during the neutralization of supergene fluids

responsible for the formation of chalcocite.

Copper, molybdenum, silver, zinc, lead, and manganese concentrations were determined in the deposit. Gold and cadmium were not detected. High concentrations of copper, molybdenum, and silver coincide with phyllic alteration. Lead, zinc, and manganese occur in normal concentrations in the deposit. Copper distribution indicates a possible extension of the main ore body at depth to the southwest.

CHAPTER II

INTRODUCTION

Porphyry copper deposits in the southwestern United States have significantly contributed to the total domestic production of copper. Arizona alone is the source of 55 percent of the copper in the nation. These deposits are attractive exploration targets because of their large size and low-cost mining characteristics. Modern discoveries of porphyry copper mineralization have utilized trace metal geochemistry and hydrothermal alteration as viable exploration tools. This investigation of the Copper Cities deposit in Arizona is based on a trace element analysis and hydrothermal alteration study of the ore body. The clay minerals present in the deposit were examined in detail in order to determine if both hypogene and supergene clay minerals exist.

Location and Mining History

The Copper Cities deposit is located in the Globe-Miami district, Gila County, Arizona, near the town of Miami (Fig. 1). The mine is in Sec. 7, T. 1 N., R. 15 E. and Sec. 12 (unsurveyed) T. 1 N., R. 14 E.

Initial mining of the deposit began in the 1890's with the exploitation of small pockets of gold and silver. The first exploration attempts for copper mineralization began in 1917 and continued through 1922 with the sinking of a shaft and 12 drill holes by the Louis d'Or Mining and Milling Company. Assay results indicated the presence of

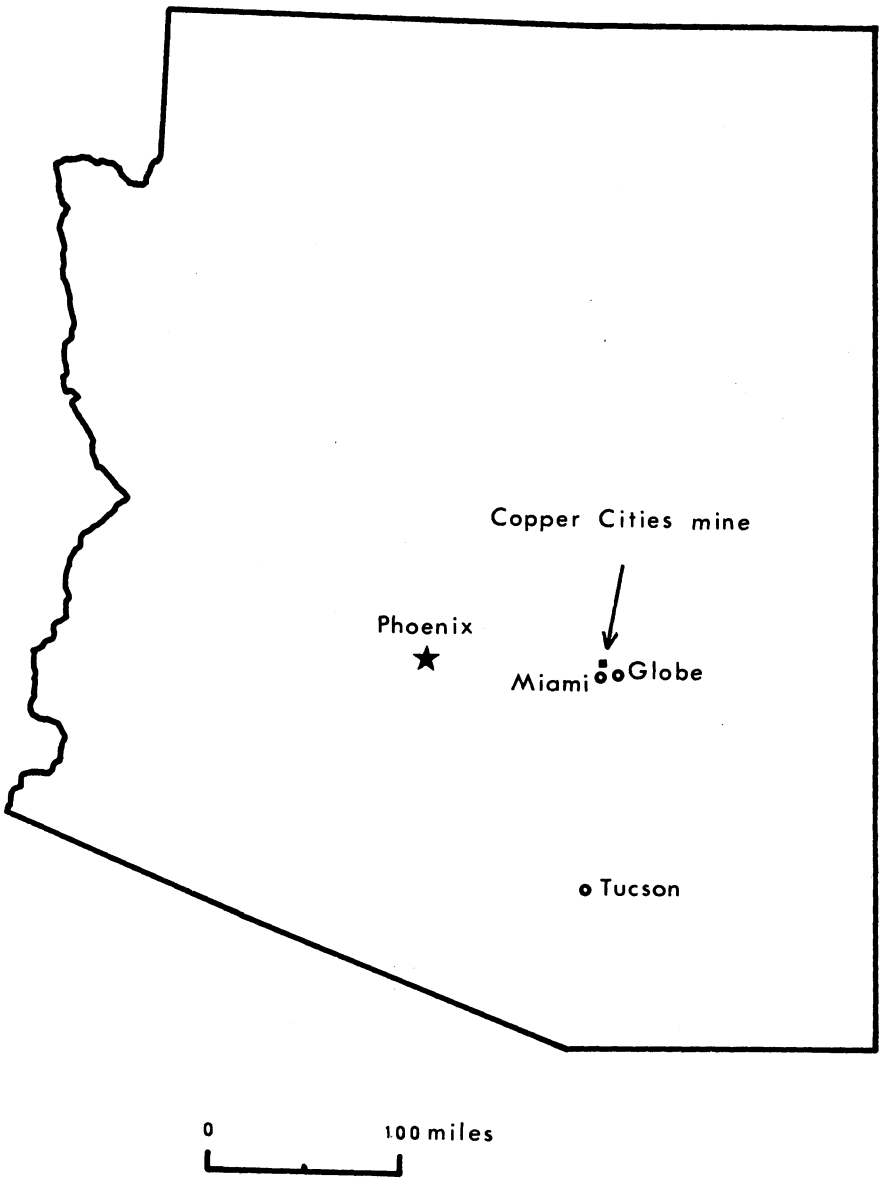

Fig. 1.-Index map of Arizona showing location of the Copper Cities mine.

low-grade copper mineralization.

The Miami Copper Company purchased the property in 1940 and conducted churn drill exploration from 1943 through 1948. An ore body of 33 million tons was delineated from assay results. Mill production began in 1954 with the acquisition of mining equipment and concentrator facilities from the depleted Castle Dome mine. The utilization of this equipment was a major factor in the decision to mine the Copper Cities deposit (Simmons and Fowells, 1966). By the end of 1962, more than 27 million tons of ore had been processed at the rate of 12,000 tons per day. Induced leaching of the 40 million tons of mine waste was begun in December, 1962.

Previous Work

The Globe-Miami district has been studied by Ransome (1903, 1919) and Peterson, Gilbert, and Quick (1951). Peterson (1954, 1962) and Simmons and Fowells (1966) reported on the Copper Cities deposit. Still (1962) studied the distribution of uranium in the Copper Cities deposit.

CHAPTER III

GEOLOGY OF THE COPPER CITIES AREA

General Setting and History

The Copper Cities area is characterized by rocks ranging in age from Precambrian to Recent (Fig. 2). The oldest unit in the area is the Pinal Schist of Lower Precambrian age. This unit represents the basement rock throughout a large portion of southeastern Arizona. The schist was intruded by the Ruin granite in Lower Precambrian time, along a northeastern trend in the northern portion of the district. This contact probably represents a zone of weakness inherited from the Precambrian (Peterson, 1962). Resting unconformably on these Lower Precambrian rocks are conglomerate, quartzite, and limestone units of the Upper Precambrian Apache group. The Apache group is overlain unconformably by Paleozoic sediments that include the Cambrian Troy quartzite and Devonian, Mississippian, and Pennsylvanian limestones.

Late Cretaceous-Early Tertiary Igneous Activity

The Late Cretaceous-Early Tertiary orogeny was initiated in the Globe-Miami district by several episodes of igneous activity.

Lost Gulch Quartz Monzonite. One of the earliest intrusions in the area was the Lost Gulch quartz monzonite. K/Ar dating methods give an age of 64 million years for the quartz monzonite (Anderson, 1968).

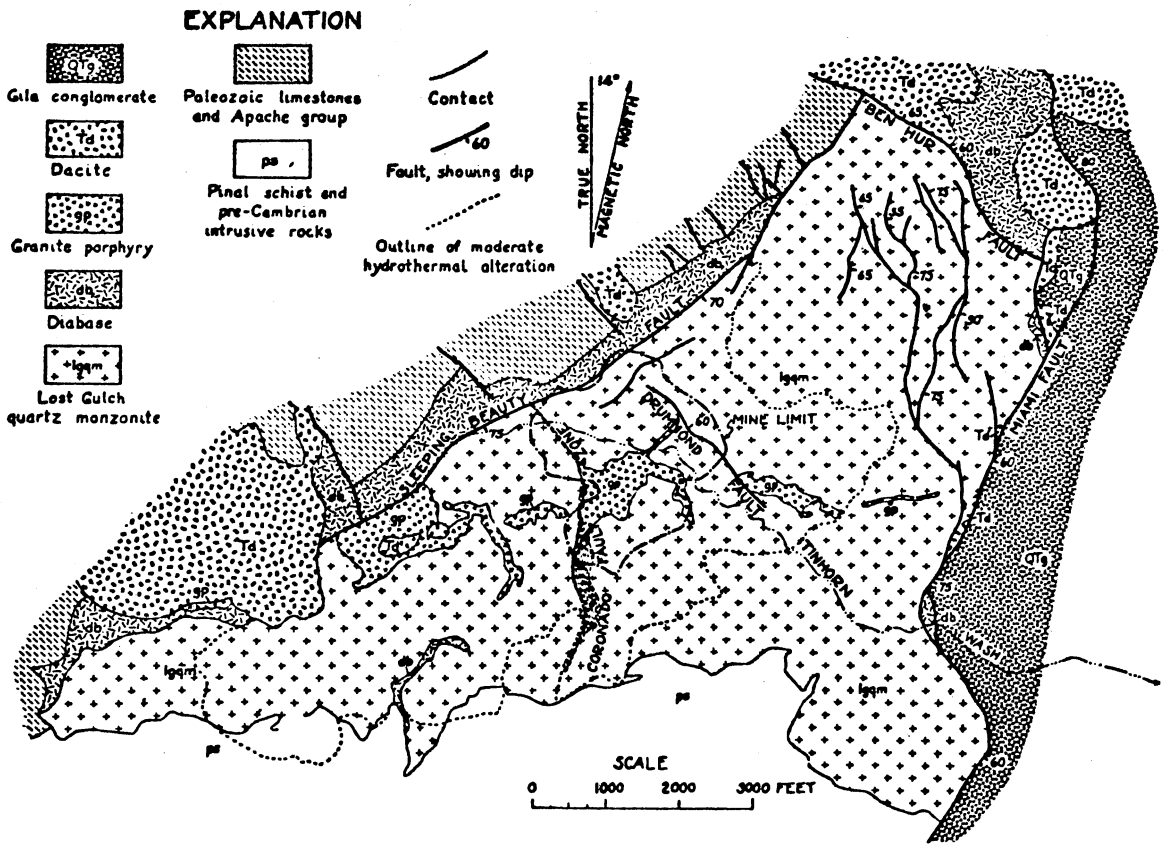

Fig. 2.-Geologic map of the Copper Cities area (from Peterson, 1954).

The quartz monzonite is the main ore host at the Copper Cities mine.

Following the emplacement of the stock, a period of widespread faulting and fracturing occurred with subsequent diabase intrusions throughout the district. The Lower Paleozoic and Precambrian rocks were extensively invaded by the diabase, both as dikes along faults and sills between strata. The Lost Gulch quartz monzonite contains several small stringers and masses of diabase exposed in the pit.

Granite Porphyry. The intrusion of granite porphyry was the next phase of igneous activity in the area. This granite porphyry is thought to be a facies of the Shultze granite which was emplaced in the southern part of the district soon after the intrusion of the Lost Gulch quartz monzonite (Peterson, 1954). Anderson (1968) gives a K/Ar date of 62 million years for the granite porphyry. This unit occurs as irregular masses aligned in an easterly trend through the quartz monzonite stock. It is not extensively mineralized or altered, suggesting that it is younger than or contemporaneous with the major influx of mineralizing fluids (Peterson, 1954).

Tertiary-Quarternary Activity

Another period of widespread faulting occurred during and after the mineralization of the Lost Gulch quartz monzonite. This was followed by continued uplift, erosion, and deposition of the Whitetail conglomerate of Tertiary age. Tertiary activity continued with the eruption of dacite which buried the district to a thickness of 1200 feet.

Another period of faulting, uplift, and erosion stripped the dacite

from parts of the district. The Quarternary Gila conglomerate is composed of material derived from this erosional episode.

Structural Geology

The Lost Gulch quartz monzonite body is a horst block trending in a northeasterly direction with normal faults forming the northwest, northeast, and east contacts. The southern limit of the quartz monzonite is a steeply-dipping intrusive contact with the Pinal schist.

The Miami fault forms the eastern boundary of the horst block and represents the contact between the Gila conglomerate and the quartz monzonite. This fault dips to the east with a throw estimated at over 1000 feet. The Miami fault is one of the more prominent structural features in the district. The Ben Hur fault, striking N45°W with a 60° dip to the northeast, is the northeast boundary of the quartz monzonite block. Diabase overlain by dacite is in contact with the quartz monzonite along this fault.

The Sleeping Beauty fault, striking northeast with a generally steep dip, is the northwest boundary of the quartz monzonite body. This fault brings sedimentary rocks of Paleozoic and Precambrian age into contact with the quartz monzonite. A thick diabase dike was intruded along this fault, with later displacement occurring along the diabase-quartz monzonite contact.

The ore body is bounded on the east and west by two fault zones which are the limits of significant copper mineralization in those directions. The Coronado fault zone, on the west, is a wide zone of shearing and brecciation striking north and dipping steeply to the west. Small lenticular bodies of diabase have intruded this zone. The

Drummond fault zone, striking N45°W and dipping 60° northeast, represents the eastern limit of significant mineralization. This fault is characterized by a narrow zone of silicified breccia. Peterson (1954) indicates that these fault zones are boundaries between two textural varieties of the Lost Gulch quartz monzonite, porphyritic quartz monzonite between the faults and quartz monzonite porphyry beyond them.

The mineralized portion of the quartz monzonite is intricately fractured by small, discontinuous faults. Simmons and Fowells (1966) noted the presence of a set of minor, persistent faults, averaging one inch in width, which parallel the contact of the granite porphyry in the northwest portion of the pit. These faults are mineralized.

Petrology

Lost Gulch Quartz Monzonite

The Lost Gulch quartz monzonite is composed of 30-35 percent quartz, 20-25 percent orthoclase, 30 percent oligoclase, and 8 percent biotite. Accessory titaniferous magnetite, apatite, zircon, and sphene are also present. Two textural varieties of the quartz monzonite have been recognized. One variety, porphyritic quartz monzonite, contains large orthoclase phenocrysts in a coarse-grained groundmass of quartz, feldspar, and biotite. The other variety, quartz monzonite porphyry, contains large phenocrysts of orthoclase and quartz in a finer-grained groundmass of quartz, feldspar, and biotite. At the Copper Cities mine, most of the ore-grade mineralization is confined principally to the porphyritic quartz monzonite. It has been determined, however, that there is no significant difference in the amount of mineralization present in the two varieties (Simmons and Fowells, 1966).

Granite Porphyry

The granite porphyry exposed in the mine contains phenocrysts of orthoclase, oligoclase, biotite, and euhedral quartz in a microcrystalline groundmass of quartz and feldspar. This granite porphyry is very similar to porphyritic bodies associated with the Shultze granite exposed elsewhere in the district. Ransome (1903) indicated that the Shultze granite is chemically a sodium-rich granite but mineralogically a quartz monzonite.

Mineralization

Primary Mineralization

The primary sulfides present in the hypogene zone of the ore body are pyrite, chalcopyrite, and minor molybdenite. The pyrite and chalcopyrite are present as individual grains in the rock and as veinlets with quartz. Molybdenite is very rare, occurring as discontinuous veinlets in the ore body. Some sphalerite and galena have been observed but only in trace amounts (Peterson, 1954).

Secondary Mineralization

Chalcocite and covellite are the only secondary sulfide minerals present in the deposit. The chalcocite formed through replacement of primary chalcopyrite and pyrite. The covellite is a replacement product of chalcocite and is found in the upper zone of the chalcocite blanket.

Malachite, azurite, and turquoise are also present in the secondary zone, malachite being the most plentiful of the three. Some very minor amounts of metatorbernite have also been seen along fractures in the

supergene zone (Simmons and Fowells, 1966).

Alteration

Peterson (1954) recognized three phases of hydrothermal alteration in the Copper Cities deposit, a quartz-sericite phase, an argillic phase, and a feeble border phase corresponding to propylitic alteration.

The quartz-sericite phase is characterized by quartz and sericite bands bordering mineralized veins and by widespread silicification. The argillic phase coincides with the development of a clay mineral of the montmorillonite group as an alteration of plagioclase. Alteration products in the outer fringe of the mineralized area include chlorite, epidote, sericite, calcite, and clinozoisite.

CHAPTER IV

SAMPLING, PREPARATIONS, AND ANALYTICAL PROCEDURES

Sampling

The field work for this study was completed during a two week period from the latter part of May through the first week of June, 1974. Samples were obtained from mine benches and diamond drill cores. The mine bench samples were collected from consecutive levels, 80 to 90 feet apart, beginning at the bottom of the pit on the 3340 foot level, to the benches in the leached capping at the 4200 foot level. The diamond drill cores were sampled at intervals roughly coinciding with the elevations of the mine benches previously sampled. The lack of available core samples from the upper levels of the mine limited this study to the 3735 through 3340 foot levels.

Sample Preparations

All samples prepared for analysis were first sliced with a diamond saw to eliminate surface contamination and crushed in a ceramic jaw crusher. A tungsten carbide Specs mill was then used to pulverize the samples to a final size of 80-mesh or smaller.

Analytical Procedures

Elemental Analysis

Total rock analysis was conducted using 1.0 gram of sample dissolved in 25 ml of concentrated hydrofluoric acid, 10 ml of concentrated nitric acid, and 2 ml of 70 percent perchloric acid in a 100 ml teflon beaker. The mixture was allowed to digest for 12 hours on a hot plate and then boiled to dryness. Two ml of distilled water and 10 ml of concentrated hydrochloric acid were next added to the yellowish-brown residue and boiled until the residue was totally dissolved. The final solution was allowed to cool and then diluted to 100 ml with distilled water.

Analysis for gold and silver required the digestion of 5.0 grams of sample in 10 ml of concentrated aqua regia. The solution was boiled to near dryness and 4 ml of distilled water was added. It was again boiled to near dryness and then filtered after cooling. The final solutions were diluted to 50 ml and transferred to polyethylene bottles.

A Perkin-Elmer 403 double-beam atomic absorption spectrophotometer was used to analyze the samples. Copper, lead, zinc, cadmium, manganese, silver, and gold were determined with an air-acetylene flame, and molybdenum concentrations were determined using a nitrous oxide-acetylene flame.

Accuracy Determinations

The accuracy attained in the trace element analyses was determined using United States Geological Survey rock standards G-2, GSP-1, AGV-1, and BCR-1. The standards were prepared for analysis following the

procedures used for the samples in the study, and were analyzed concurrently. Table I is a comparison of the data obtained in this study and the values derived from U.S.G.S. analyses of the standards (Flanagan, 1969). Molybdenum values show a greater variation from the mean for low concentrations. Silver could not be detected in the standards.

Clay Mineral Analysis and Identification

Oriented slides for X-ray analysis were prepared using a portion of the minus 80-mesh fraction of the samples. The sample was mixed with distilled water and allowed to settle for 30 minutes. The clay-sized particles were removed from the upper one-half centimeter of the mixture with a pipette and transferred to ceramic X-ray slides. A Phillips X-ray diffraction unit using Cu K-alpha radiation scanned the samples over the interval 2 through 30 degrees 2 Θ at a rate of 1 degree 2 Θ per minute.

Identification and semiquantitative analysis of the clay minerals followed methods described by Carroll (1970), Brown (1961), and Weaver and Pollard (1973). The clay percentages represent fractions of the total clay mineral content in each sample. Heat treatments and glycolation were used to verify clay mineral identifications.

Sericite. Sericite, or fine-grained dioctahedral mica, is identified by the presence and intensity of its 002 and 004 reflections at 9.9Å and 4.9Å respectively (Fig. 3). The reflections are not affected by glycolation or heat treatments. The sharpness of these reflections is indicative of high-temperature 2M illite. Broad peaks are more characteristic of 1M or 1Md illite which are formed in lower-energy environments (Carroll, 1970).

TABLE I

COMPARISON OF PUBLISHED MEAN VALUES[1] WITH THE PRESENT STUDY'S VALUES FOR U.S.G.S. STANDARDS G-2, GSP-1, AGV-1, AND BCR-1

Element[2]	G-2 USGS	G-2 Present Study	GSP-1 USGS	GSP-1 Present Study
Ag	0.04	-	0.07	-
Cu	11	10	35	42
Mn	265	256	326	308
Mo	1.2	4	1.6	5
Pb	29	50	52	76
Zn	74	118	143	132

Element[2]	AGV-1 USGS	AGV-1 Present Study	BCR-1 USGS	BCR-1 Present Study
Ag	0.1	-	0.04	-
Cu	63	69	22	20
Mn	728	742	1350	1348
Mo	4	6	4	5
Pb	35	50	18	20
Zn	112	100	132	148

[1] Flanagan, 1969

[2] Parts per million

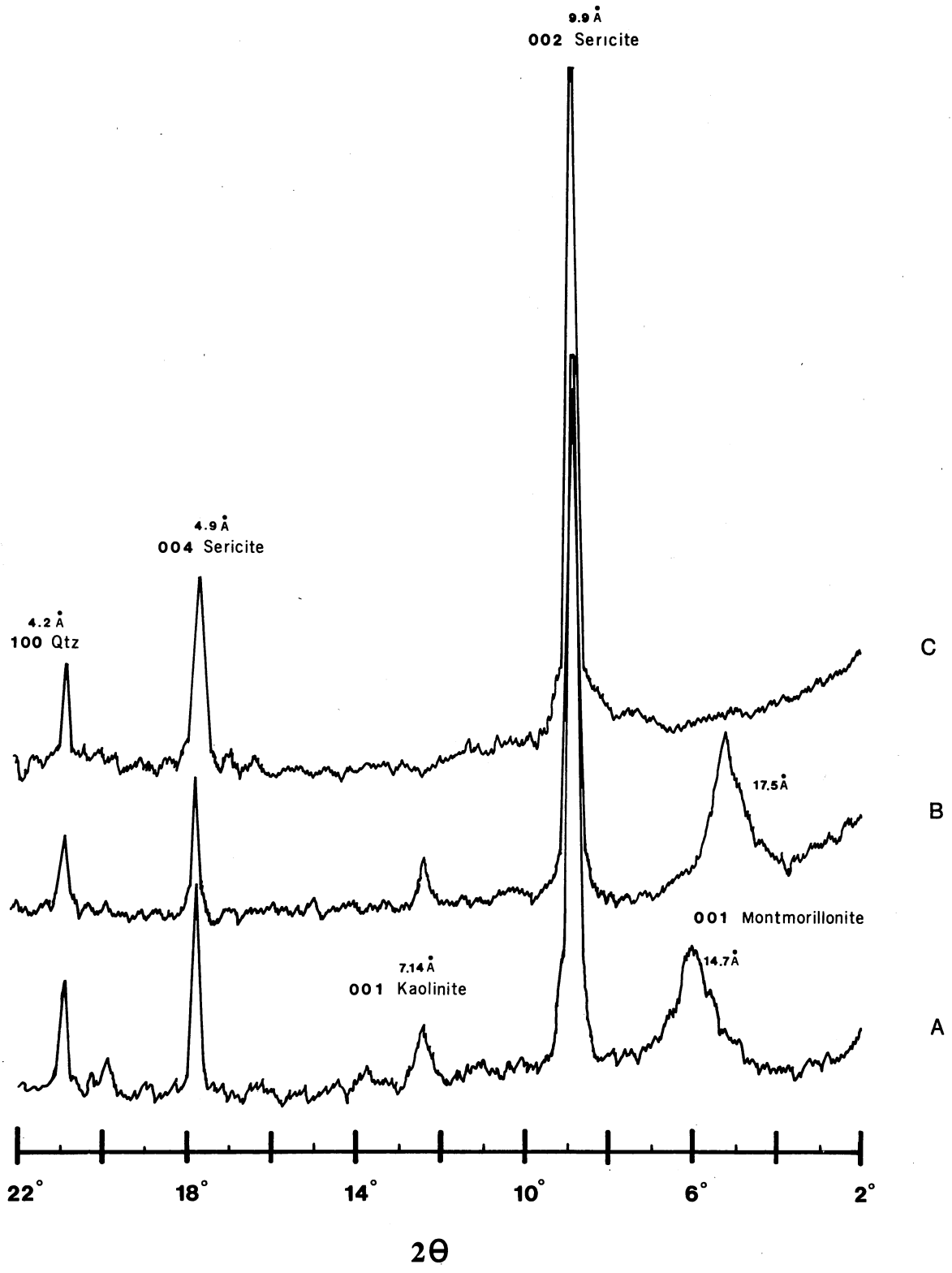

Fig. 3.-X-ray diffraction charts of sample DDH 510 - 3645 showing A) no treatment, B) glycolation for 24 hours, and C) heat treatment - 600°C for 1 hour.

Further X-ray diffraction analysis was carried out to determine if differences in the structure of sericite occur between hypogene and supergene environments. Samples from the 3340 foot level to the 3735 foot level of three diamond drill cores were X-rayed. The intensities of the 002 and 004 basal reflections were used to calculate the ratio: $I_{002}/I_{002} + I_{004}$. The value of this ratio will increase with a decrease in the 004 intensity, indicating a gradual disruption of the sericite crystal structure. This disordered structure is characteristic of a low-temperature, or supergene environment of formation. Results from the core samples are given in Table II. No significant vertical variation in the intensity ratios is present. Therefore, no apparent transformation of hypogene sericite to a disordered form in the supergene zone could be detected in the deposit.

Montmorillonite. Montmorillonite has a first order basal reflection at 14.7Å. After a 24 hour treatment in an atmosphere of ethylene glycol, the basal spacing was expanded to 17.5Å (Figs. 3, 4). These (001) reflections indicate that calcium is the interlayered cation. From studies of argillic facies in porphyry copper systems, Burnham (1962) concluded that calcium is the most common interlayered cation in hydrothermal montmorillonite. Peterson et al. (1946) reported that the hypogene montmorillonite present in the Castle Dome deposit, six miles southwest of the Copper Cities mine, contained calcium as an exchangeable base.

Several studies of porphyry copper deposits have dealt with the question of a hypogene versus supergene origin of montmorillonite. Burnham (1962) believes that montmorillonites in porphyry copper systems are of hypogene origin. The same conclusion was drawn by Shepard et al.

TABLE II

X-RAY PEAK INTENSITY RATIOS OF SERICITE[1], COPPER CITIES DEPOSIT

Elevation (Ft.)	Diamond Drill Holes 503	506	333
3735	.77	.77	.81
3645	.82	.83	.81
3550	.75	.84	.78
3460	.75	.79	.79
3380	.83	.79	.75
3340	.72	.74	.83

[1]Computed from the formula: $I_{002}/I_{002} + I_{004}$.

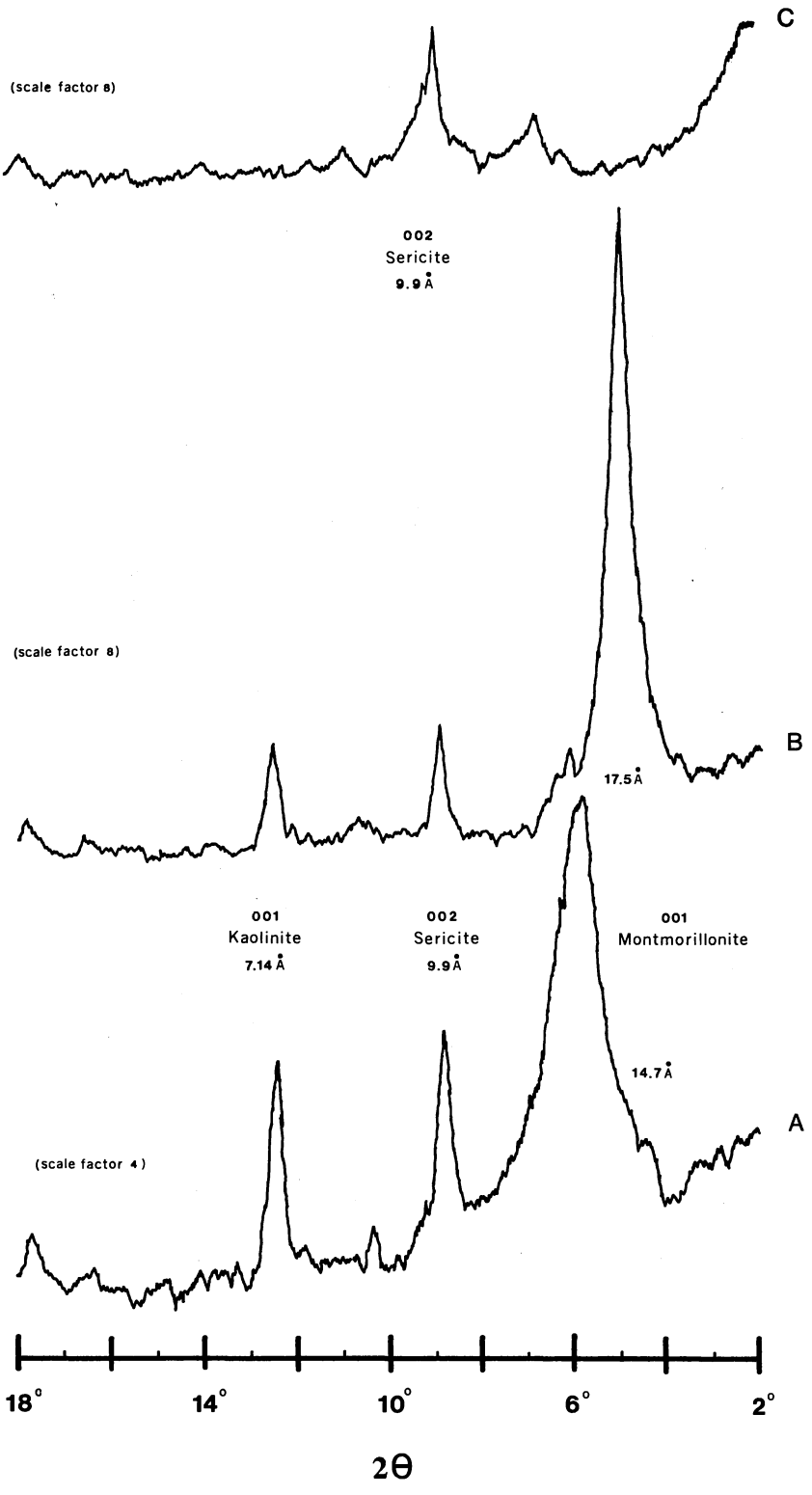

Fig. 4.-X-ray diffraction charts of sample PS-14 showing A) no treatment, B) glycolation for 24 hours, and C) heat treatment - 600°C for 1 hour.

(1969) from isotope ratio data involving clay samples from several porphyry copper deposits. The similarity of the montmorillonite in the Copper Cities deposit to published descriptions of hypogene montmorillonites indicates that the montmorillonite is probably hypogene.

Kaolinite. The first order basal reflection of kaolinite occurs at 7.14Å. This first order reflection is destroyed by a heat treatment of 600°C for 1 hour (Figs. 3, 4). This technique was used to differentiate the 001 kaolinite reflection from the 002 chlorite reflection which occurs at 7.13Å (Carroll, 1970). Chlorite is unaffected by heating, but the kaolinite structure is destroyed by the loss of hydroxyl ions at elevated temperatures. No other 1:1 clay minerals such as dickite were recognized in samples from the deposit.

CHAPTER V

RESULTS AND DISCUSSIONS

Data from clay mineral and trace element analyses are presented and discussed in the following sections. Both plan view and cross section maps of the deposit are included in the discussions. An index map of the mine (Fig. 5) shows the locations of the pit benches and cross sections utilized in these maps.

Clay Mineral Distribution

The distribution patterns of the clay minerals are shown in cross section in Figures 6 and 7, and in plan view in Figures 10, 11, and 12 (in pocket). The zone of greater than 50 percent sericite indicates maximum sericitic alteration. The majority of samples from this zone contain 75 percent or more sericite. The 50 percent value for montmorillonite and the 30 percent value for kaolinite were chosen to represent significant changes in the alteration assemblages. Kaolinite is the least abundant clay mineral followed by montmorillonite and sericite. Generalized cross sections of the geology in the deposit (Figs. 8, 9) are included for comparison with the other cross sections.

Sericite

The zone of greater than 50 percent sericite is an elongated body trending approximately north-south and narrowing with depth (Figs. 6,

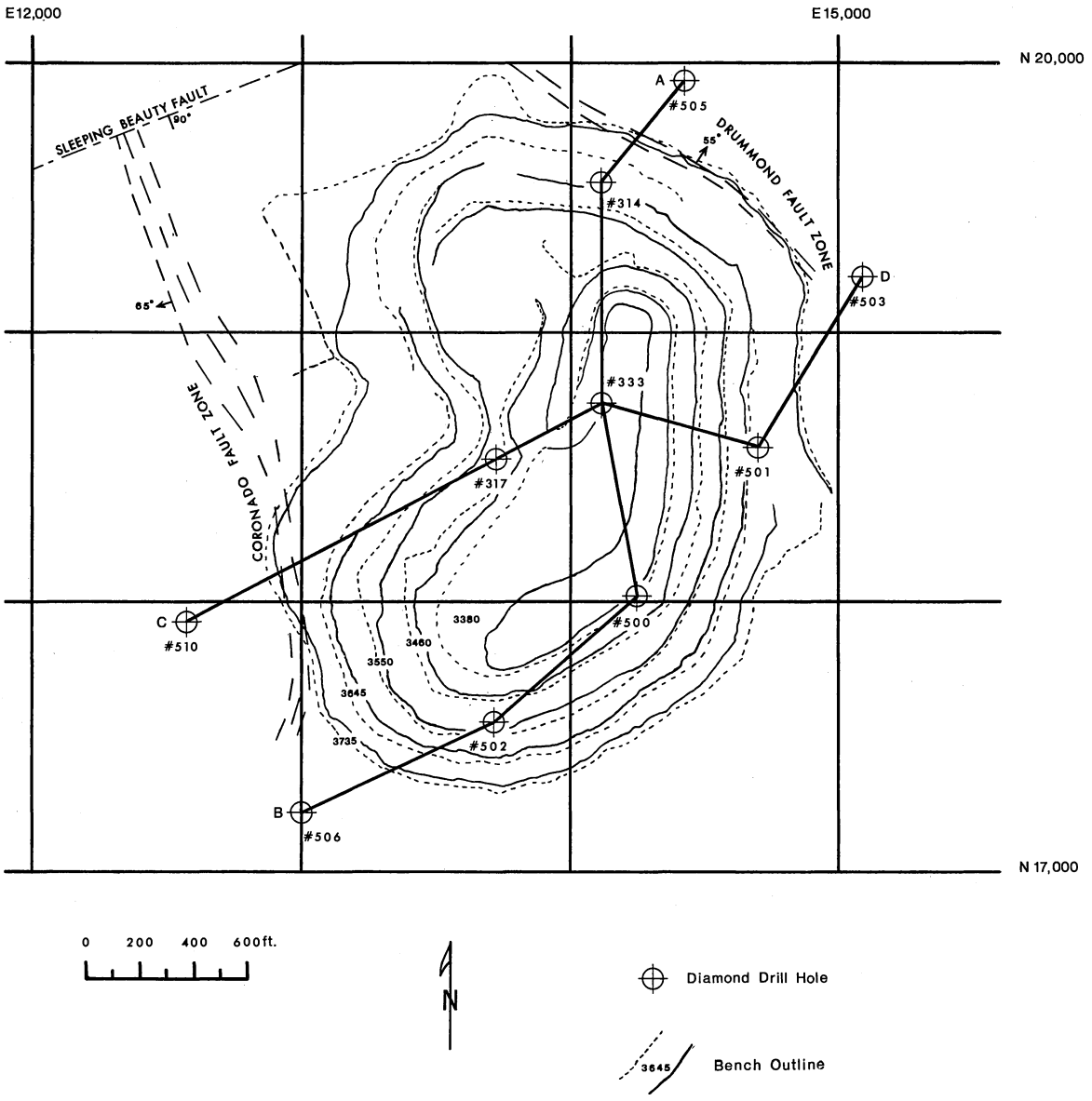

Fig. 5.-Index map of the Copper Cities mine showing cross sections A-B and C-D and selected mine benches.

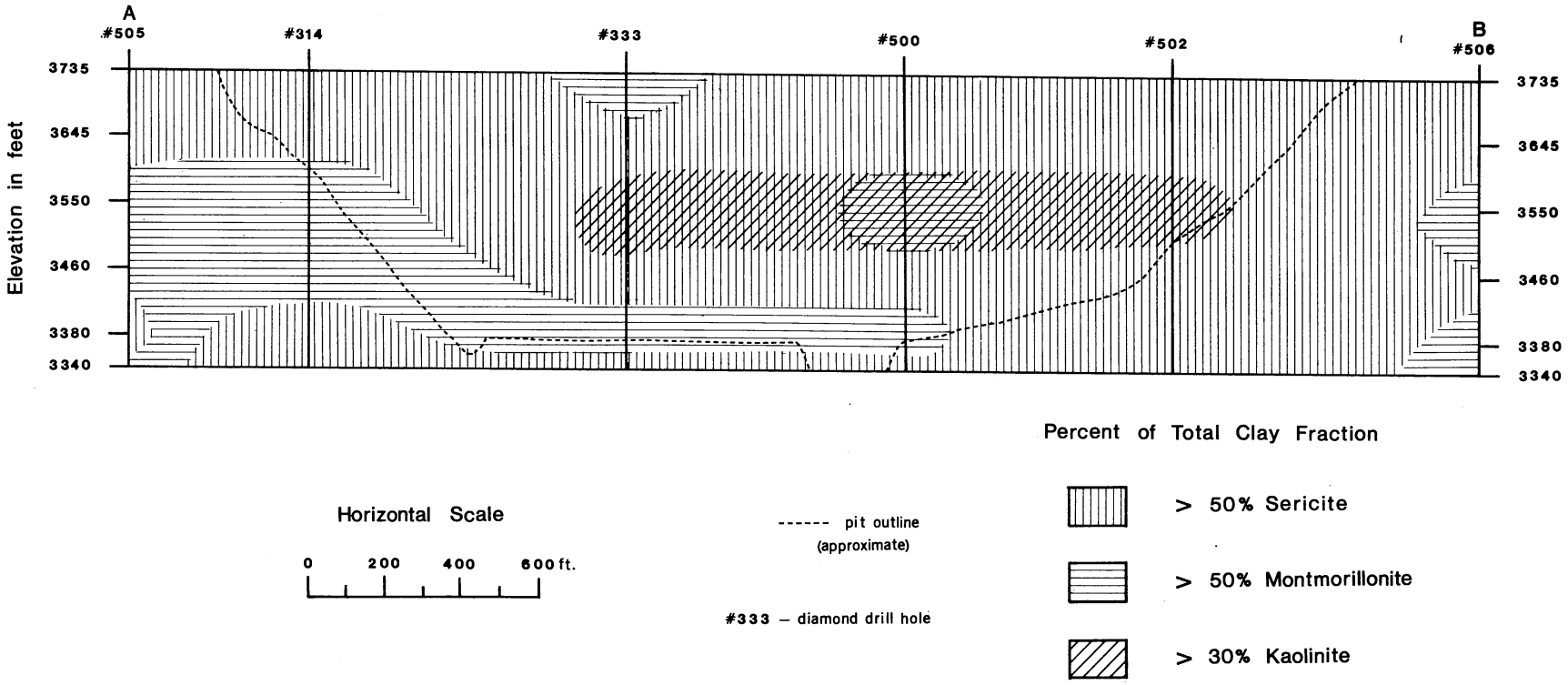

Fig. 6.-Clay mineral distribution along section A-B, Copper Cities deposit, Arizona.

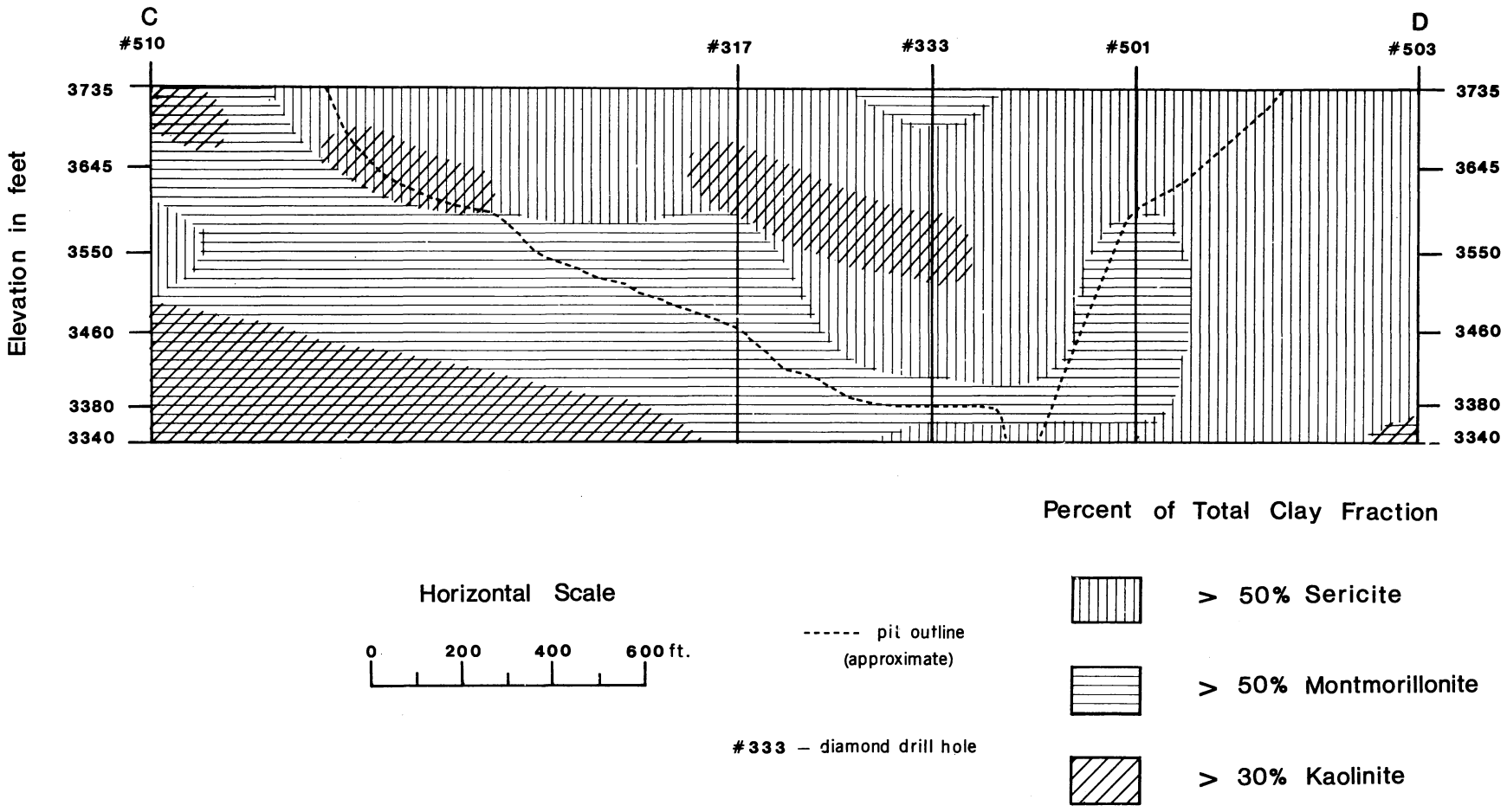

Fig. 7.-Clay mineral distribution along section C-D, Copper Cities deposit, Arizona.

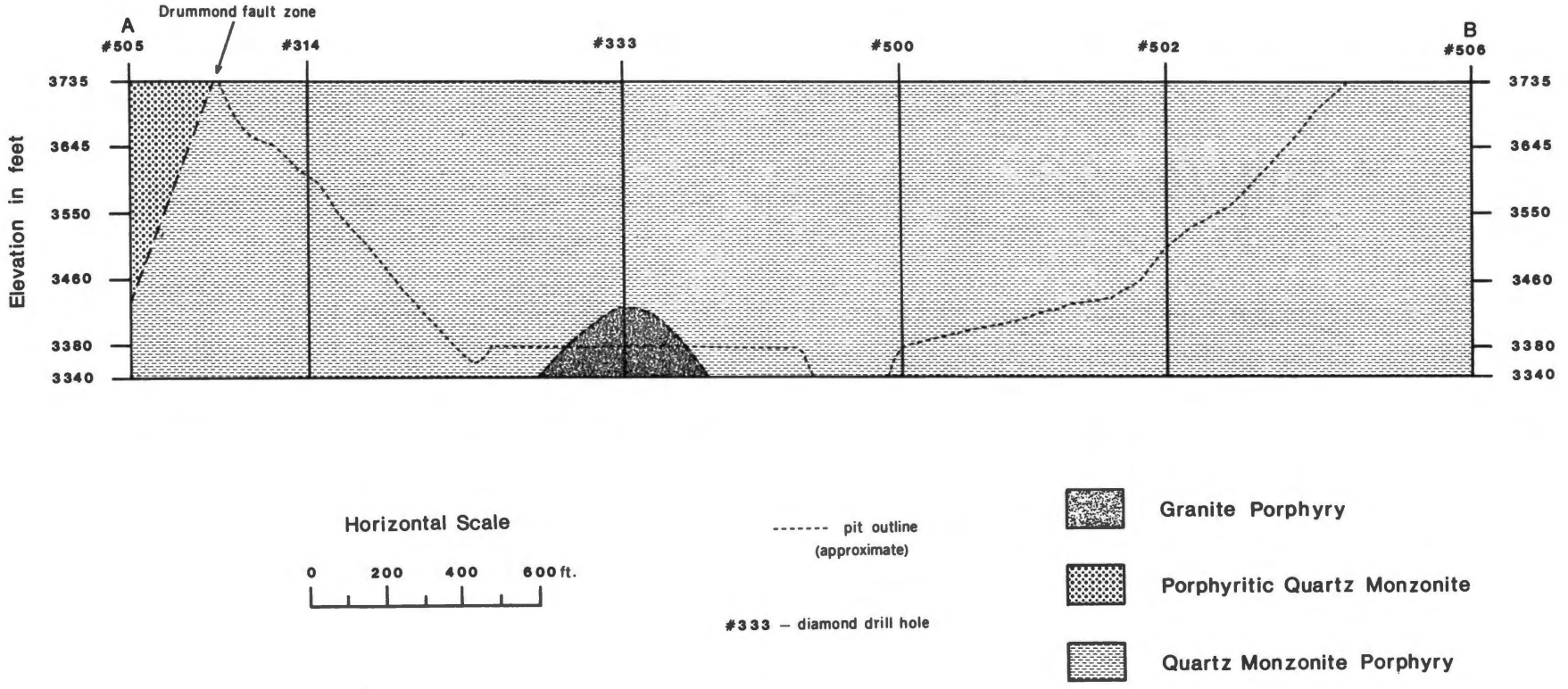

Fig. 8.-Generalized geology along section A-B, Copper Cities deposit, Arizona.

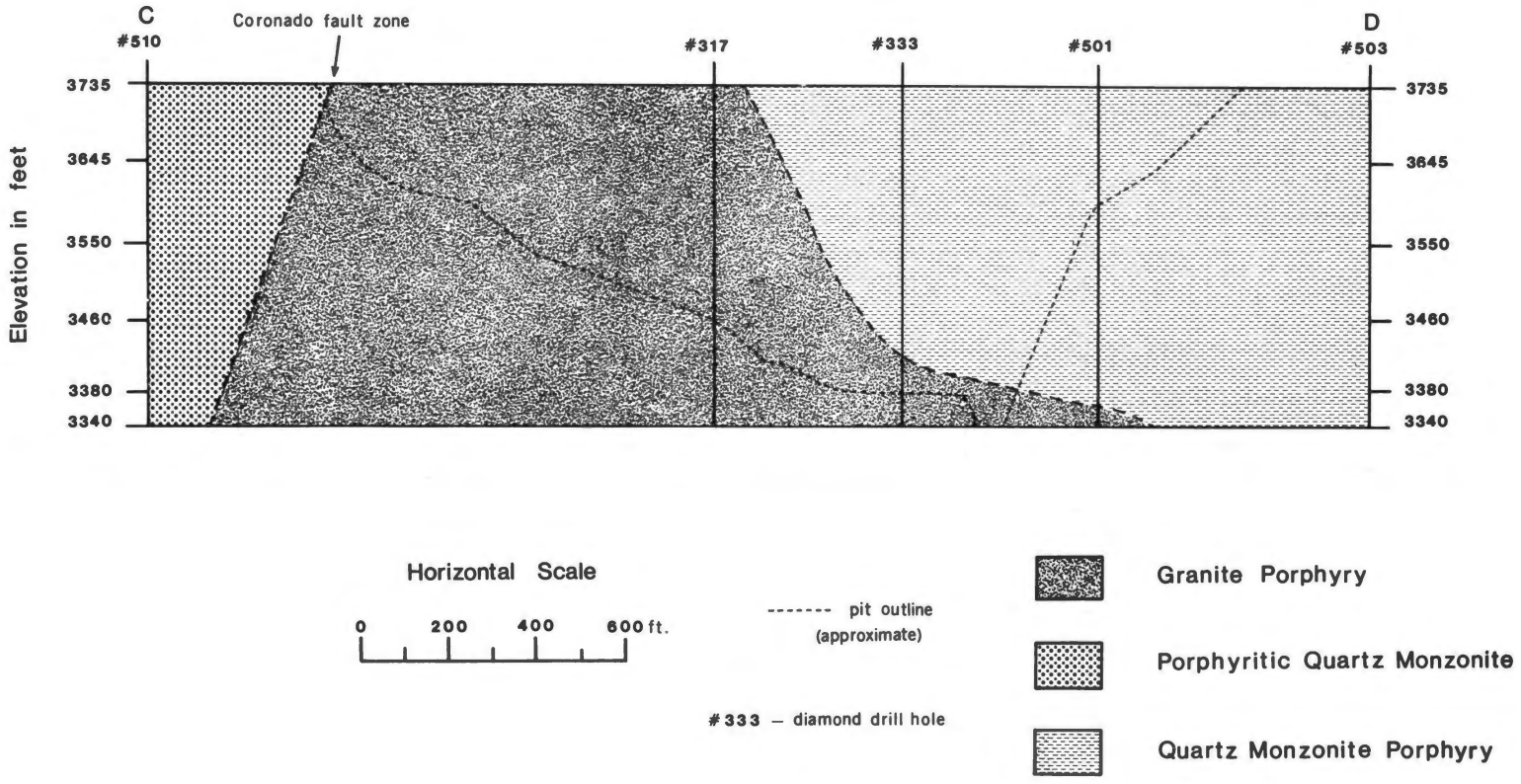

Fig. 9.-Generalized geology along section C-D, Copper Cities deposit, Arizona.

7, 10, 11, 12). Sericite is less abundant in the granite porphyry on the west and is restricted almost exclusively to the quartz monzonite (see Figs. 8, 9). The major portion of the copper mineralization occurs in the sericite zone, as shown by the pit outlines on the maps.

Montmorillonite

Figures 6, 7, 10, 11, and 12 show the distribution of montmorillonite in the mine area. It occurs in a rougly concentric zone around the central sericite core of the deposit. Of the total clay content in the granite porphyry, over 50 percent is montmorillonite. The montmorillonite is an alteration product of plagioclase in the rock.

Kaolinite

Two distribution patterns of kaolinite are readily discernible from the maps: 1) Figures 11 and 12 show kaolinite associated with montmorillonite in the argillic zone surrounding the central sericite core, 2) Figures 6, 7, and 10 show the same kaolinite-montmorillonite association along with another distribution pattern. This second pattern is in the shape of a blanket dipping to the east-southeast from the 3645 foot level of the pit to the 3550 foot level (Fig. 7). The long dimension of the pit can be seen in Figure 6.

The origin of this kaolinite "blanket" appears to be related to supergene activity. Burnham (1962) noted that porphyry copper deposits with sizeable supergene enrichment are also kaolinite-rich, while those deposits with less intense or widespread supergene enrichment such as Ajo, Bingham, and Ely were correspondingly kaolinite-poor. Anderson (1950) describes kaolinite of probable supergene origin in the Bagdad

porphyry copper deposit. This is further supported by the work of Shepard et al. (1969) involving the identification of supergene kaolinite at Santa Rita, New Mexico using D/H and O^{18}/O^{16} isotope ratios. Rose and Baltosser (1966) had previously postulated that much of the kaolinite at Santa Rita was formed by supergene processes.

The formation of the kaolinite "blanket" is related to the copper enrichment process in the supergene zone. Chalcopyrite reacts with downward percolating meteoric water in the oxidizing zone releasing copper according to the reaction:

$$2CuFeS_2 + 8.5O_2 + 2H_2O \rightarrow Fe_2O_3 + 2Cu^{+2} + 4H^+ + 4SO_4^{-2}$$

The dissolved Cu^{+2} will be carried downward by ground water and come in contact with primary sulfide minerals below the zone of oxidation. Copper sulfides are less soluble than other sulfides, thus chalcocite will form as a result of the following reaction (Krauskopf, 1968):

$$5FeS_2 + 14Cu^{+2} + 12H_2O \rightarrow 7Cu_2S + 5Fe^{+2} + 24H^+ + 3SO_4^{-2}$$

The resultant H^+ ions will react with sericite to produce kaolinite:

$$2KAl_3Si_3O_{10}(OH)_2 + 2H^+ + 2H_2O \rightarrow 3Al_2Si_2O_5(OH)_4 + 2K^+$$

The potassium ions released in the reaction will be flushed from the system by ground water.

Thus it can be seen that the formation of supergene kaolinite is directly related to the production of chalcocite.

Hydrothermal Alteration Zones

Hydrothermal alteration zones represent characteristic mineral assemblages which have formed in response to gradual changes in the temperature, pressure, and chemistry of ore forming fluids. Figure 13 shows the patterns of three hydrothermal alteration zones in the Copper Cities deposit. The determination of these zones was based on semi-quantitative analysis of the clay minerals using X-ray diffraction. Hand specimen staining with a 10 percent solution of sodium cobaltinitrite and thin section analysis were also used.

Potassic Alteration

Potassic alteration, as described by Hemley and Jones (1964), Creasy (1966), Meyer and Hemley (1967), and Lowell and Guilbert (1970), is characterized by the formation of secondary potassium feldspar and biotite. Early hydrothermal fluids in this zone were at a high enough temperature to prevent the dissociation of HCl, thereby increasing the concentration of K^+ to produce secondary potassium feldspar. This high K^+/H^+ ratio needed for the formation of potassium feldspar is illustrated in Figure 14.

The potassium feldspar, identified using a sodium cobaltinitrite stain, occurs as primary phenocrysts and secondary veinlets in the rock. Thin-section analyses indicate that secondary biotite is present as veinlets of small crystals and as large agglomerations of individual books. The potassic alteration zone forms a deep, central core below the deepest limits of the ore body (Fig. 13).

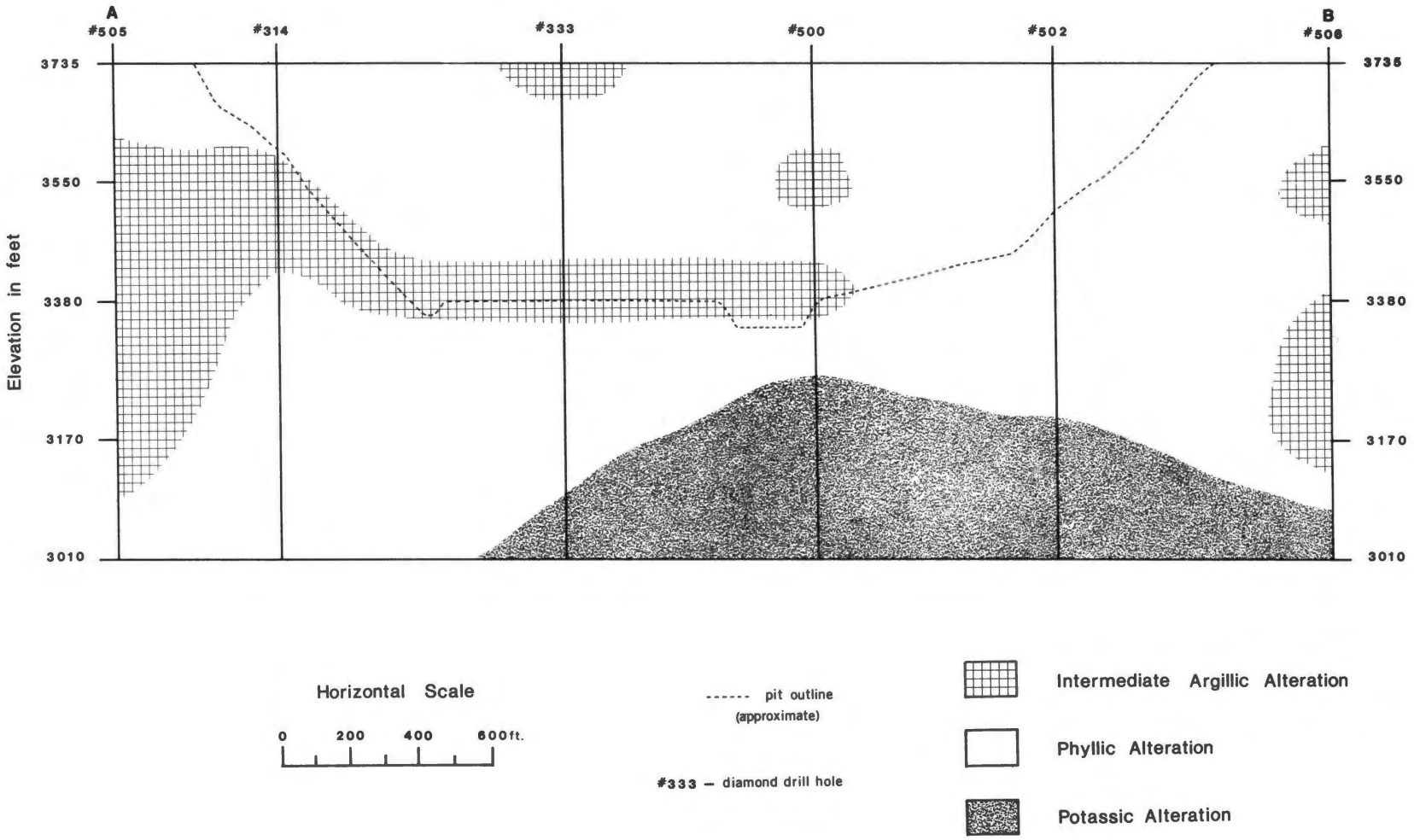

Fig. 13.-Hydrothermal alteration zones along section A-B, Copper Cities deposit, Arizona.

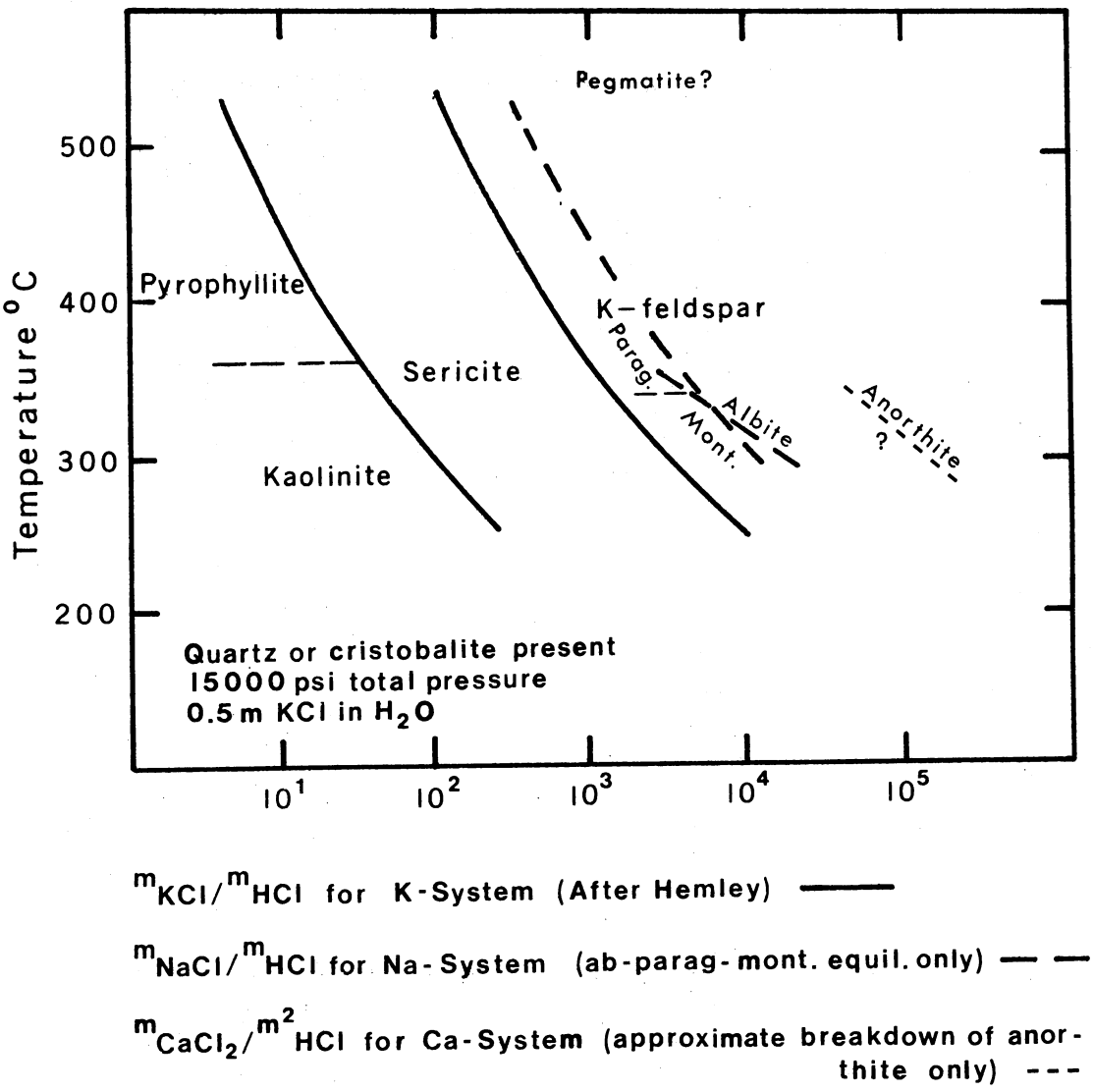

Fig. 14.-Experimental reaction equilibria for minerals in the system K_2O-Al_2O_3-SiO_2-H_2O in 0.5 molal KCl solution (after Meyer et al., 1968).

Phyllic Alteration

The phyllic alteration zone, described by Lowell and Guilbert (1970), is the zone of maximum sericitic alteration. This alteration represents the increase of H^+ activity with the gradual decrease in temperature outward from the potassic core. Potassium feldspar is commonly altered to sericite and quartz in the presence of H^+:

$$3KAlSi_3O_8 + 2H^+ \rightarrow KAl_3Si_3O_{10}(OH)_2 + 6SiO_2 + 2K^+$$

This alteration zone contains the maximum copper mineralization in the deposit.

Intermediate Argillic Alteration

The next zone outward from phyllic alteration is the intermediate argillic zone (Meyer and Hemley, 1967). Decreasing temperatures with corresponding increases in H^+ activity caused intense base leaching and the formation of kaolinite and montmorillonite:

$$Na_2CaAl_4Si_8O_{24} + 4H^+ + 2H_2O \rightarrow 2Al_2Si_2O_5(OH)_4 + 4SiO_2 + 2Na^+ + Ca^{2+}$$

(alteration of plagioclase (andesine) to kaolinite and quartz with the release of sodium and calcium ions)

The alteration of plagioclase (andesine) will also produce montmorillonite:

$$Na_2CaAl_4Si_8O_{24} + 4H^+ \rightarrow 2Ca_{.33}Al_2Si_4O_{10}(OH)_2 + 2Na^+ + Ca_{.33}^{+2}$$

In the Copper Cities deposit, the intermediate argillic zone occurs

laterally on the fringes of the phyllic zone. Figure 4 shows a typical X-ray diffraction pattern of a sample selected from this zone.

Propylitic Alteration

The propylitic alteration zone (not included in this study) is also found at the Copper Cities deposit (Peterson, 1954). The alteration is the result of weak H^+ activity during the dilution of hydrothermal fluids by ground water. Chlorite is a common alteration product in this zone:

$$2K(Mg,Fe)_3AlSi_3O_{10}(OH)_2 + 4H^+ \longrightarrow$$

$$Al(Mg,Fe)_5AlSi_3O_{10}(OH)_8 + (Mg,Fe)^{+2} + 2K^+ + 3SiO_2$$

(alteration of biotite to chlorite in the presence of H^+)

This zone grades outward from the intermediate argillic zone into fresh rock.

Copper Distribution

The mean copper value from analyzed samples is .35 percent. A value of around .4 percent was determined by Peterson (1954). The distribution of the copper mineralization is shown in Figures 15 and 16, and in Figures 10, 11, and 12 (in pocket). The ore body is funnel-shaped, narrowing with depth (Figs. 15, 16). Mineralization is significantly restricted to the area between the Coronado and Drummond fault zones (see Fig. 5). The copper mineralization is concentrated along the intrusive contact between the granite porphyry and quartz monzonite (see Figs. 8, 9). Copper content is greater in the quartz monzonite

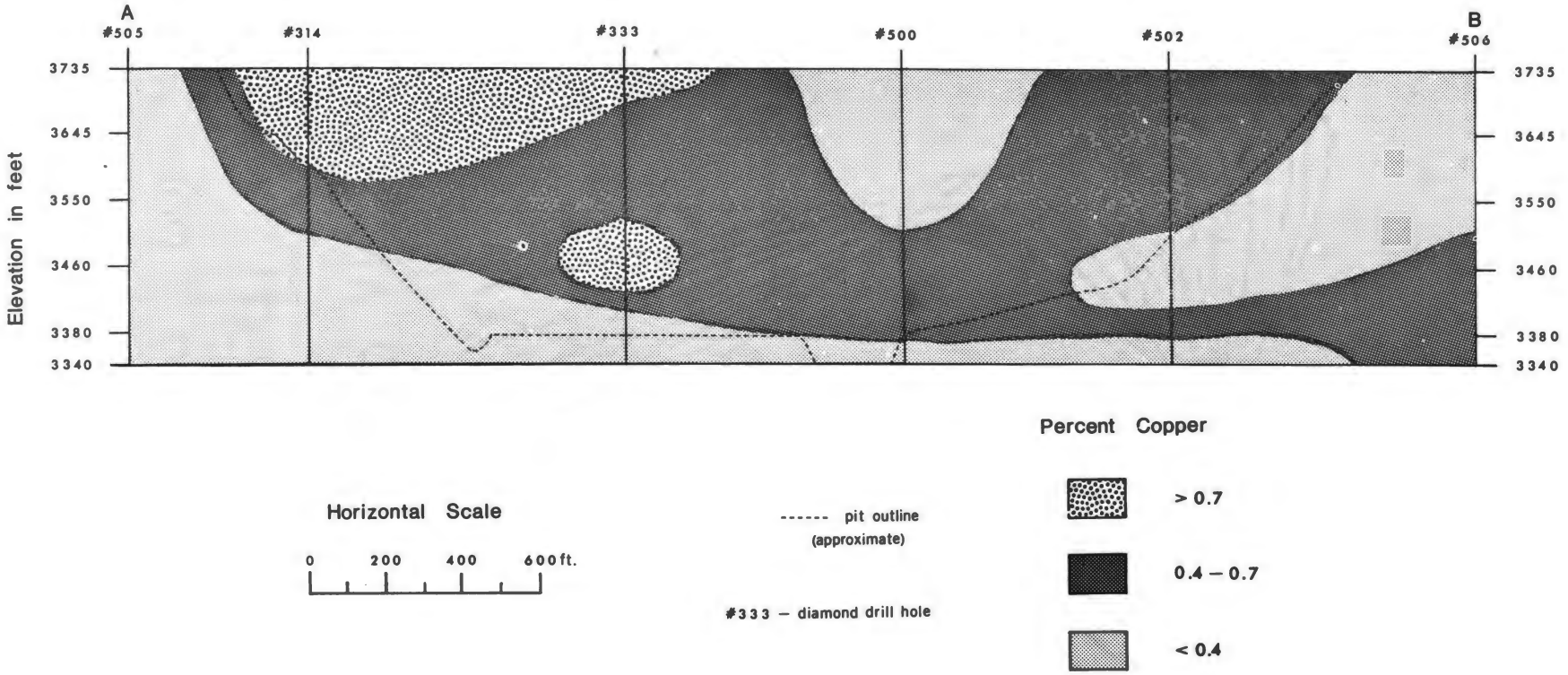

Fig. 15.-Copper distribution along section A-B, Copper Cities deposit, Arizona.

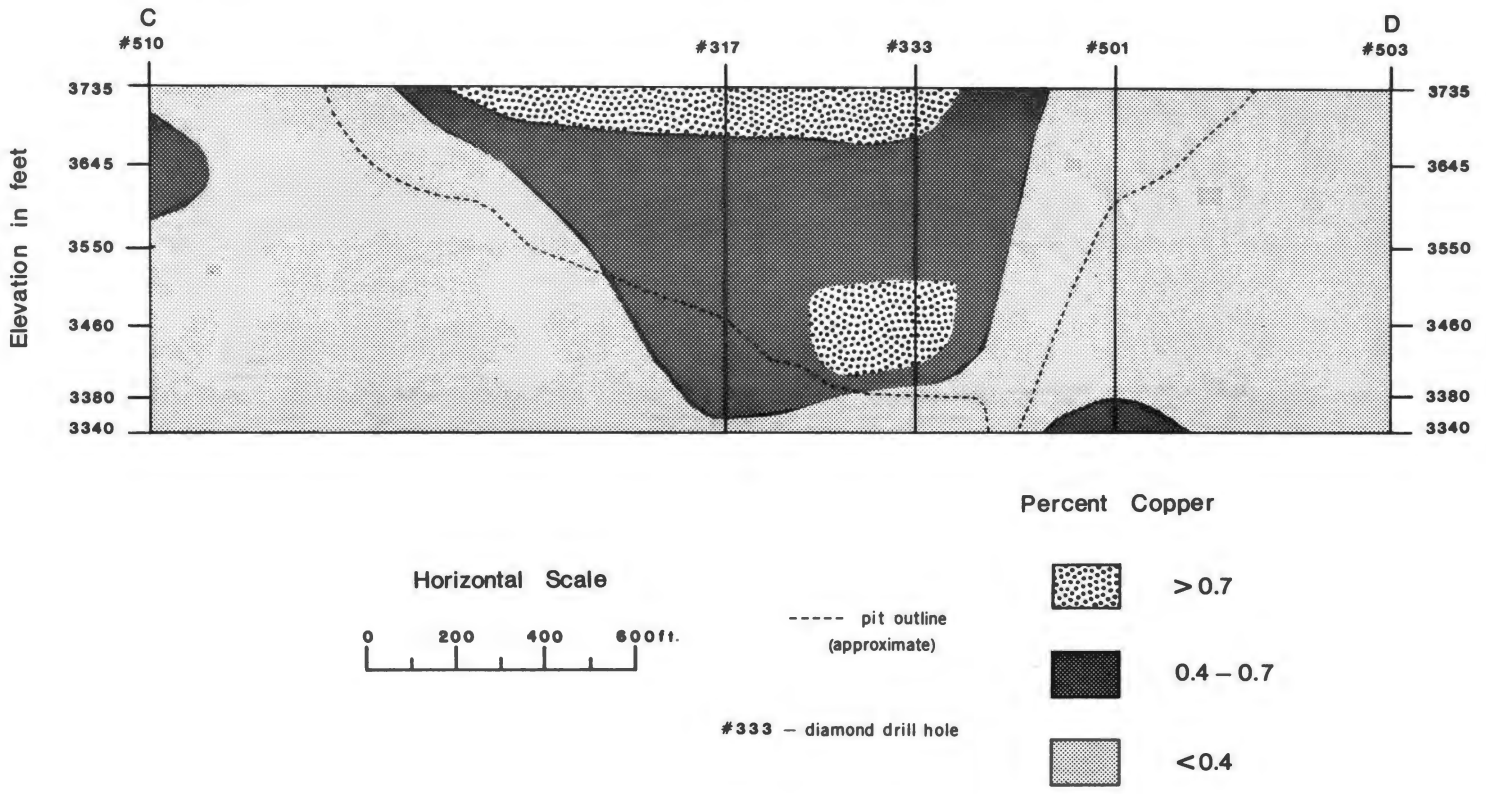

Fig. 16.-Copper distribution along section C-D, Copper Cities deposit, Arizona.

than in the granite porphyry. Copper distribution on the 3460 and 3340 foot levels of the deposit (Figs. 11, 12) shows a significant trend toward the southwest. This trend could possibly indicate an increase in mineralization southwest of the deposit as an extension of the main ore body at depth.

A comparison of Figures 6 and 15, and Figures 7 and 16 shows that the copper mineralization is spatially associated with the phyllic alteration zone. This correlation has been documented in numerous published accounts of porphyry copper systems (Meyer and Hemley, 1967, Lowell and Guilbert, 1970).

Supergene enrichment in the Copper Cities deposit is incomplete. Chalcocite is present only as coatings on chalcopyrite and pyrite grains. This partial replacement exists as deep as the 3460 foot level of the pit, along the granite porphyry-quartz monzonite contact.

Figures 15 and 16 show a zone of greater than .7 percent copper along the 3735 foot and 3645 foot levels of the pit. The high copper content in this zone is the result of supergene enrichment. The zone is slightly thicker in the quartz monzonite than in the granite porphyry because of a higher primary copper content and greater permeability of the quartz monzonite (Peterson, 1954).

Another zone of greater than .7 percent copper occurs on the 3460 foot level. Although chalcocite was seen as a minor coating on some chalcopyrite grains, the high copper grade is due to primary copper mineralization.

These two zones are separated by the kaolinite blanket shown in Figure 7. This blanket forms a boundary between the zone of progressive supergene enrichment and the zone of hypogene mineralization. Peterson

(1954) concluded from his studies of the ground-water table and of supergene enrichment that this enrichment is related to the present erosional cycle. He found that the ground-water table has a southeastern gradient and is higher in the granite porphyry than in the quartz monzonite. Figure 17 represents a generalized northwest-southeast cross section parallel to the gradient of the ground-water table. The diagram shows the position of the kaolinite blanket in relation to the zones of primary and secondary copper mineralization and the ground-water level. If the kaolinite blanket is of supergene origin, then it should be influenced by the factors controlling the orientation of the ground-water table, such as regional gradient and permeabilities of the host rocks. This, in fact, appears to be the case.

Trace Element Distribution

The distribution of trace elements in the Copper Cities deposit is shown in Figures 10, 11, and 12 (in pocket). Molybdenum, silver, lead, zinc, and manganese were determined and calculated in parts per million. Cadmium and gold were not detectible in the analyzed samples. Table III shows the metal content ratios of the plus 80 versus minus 80-mesh fractions of selected samples from the deposit. Microscopic examination of the plus 80-mesh fraction indicates that quartz, potassium feldspar, and biotite fragments constitute the coarse fraction of the samples. Figures 18 and 19 are histograms of the trace elements and copper in the deposit. Copper values are reported in percents.

Molybdenum

Guilbert and Lowell (1974) gave an average value of .015 percent

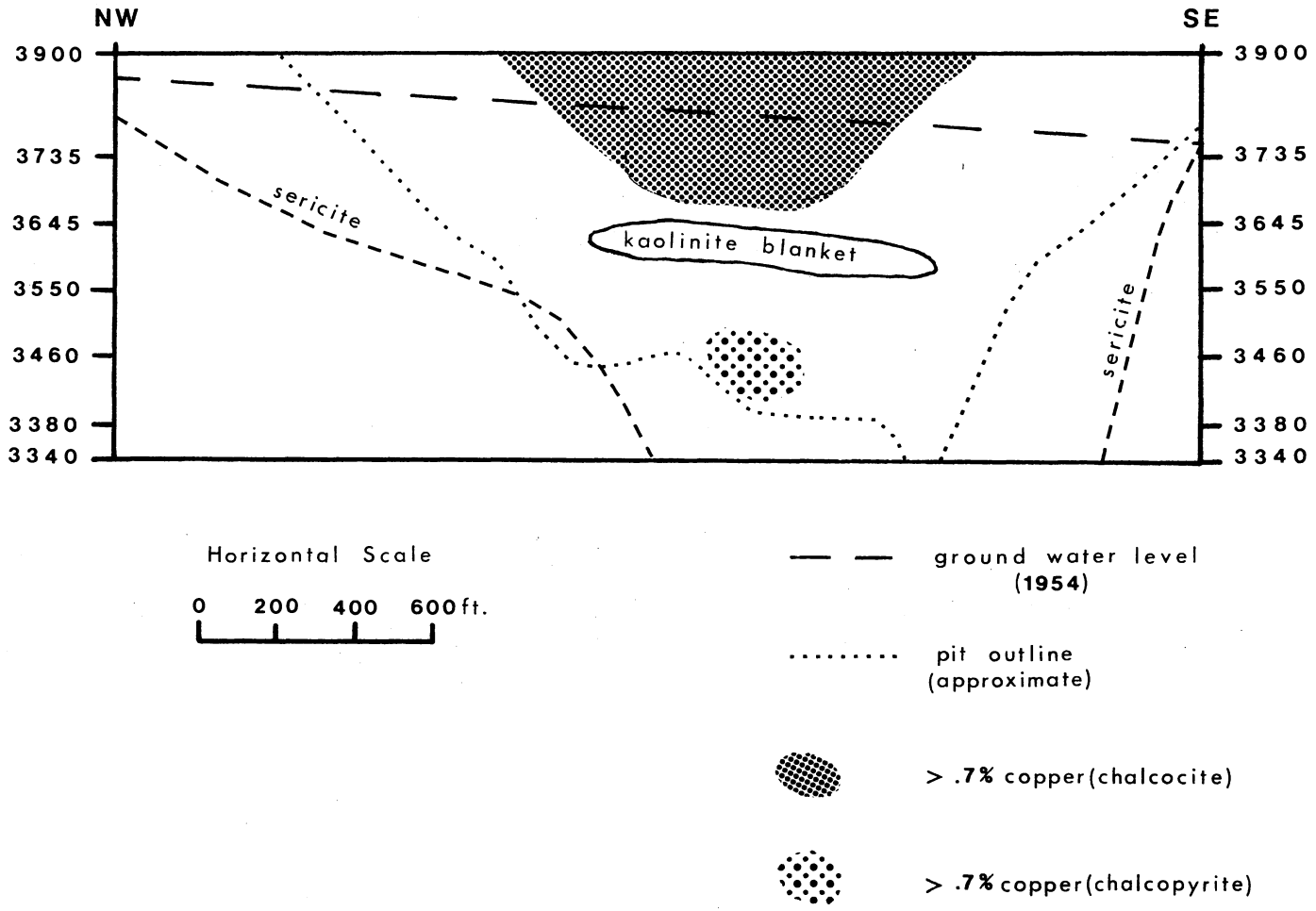

Fig. 17.-Generalized northwest-southeast cross section through the Copper Cities deposit, showing the location of the supergene kaolinite blanket in relation to copper mineralization and the ground-water level.

TABLE III

METAL CONTENT RATIOS OF THE MINUS 80 VERSUS PLUS 80-MESH FRACTIONS OF SELECTED SAMPLES[1], COPPER CITIES DEPOSIT

Ag	Cu	Mn	Mo	Pb	Zn
1:.35	1:.25	1:.45	1:.31	1:.75	1:.66

[1]Samples DDH 503 - 3340, DDH 314 - 3340, PS-17, PS-19, PS-32, PS-35, PS-40, PS-42, PS-44.

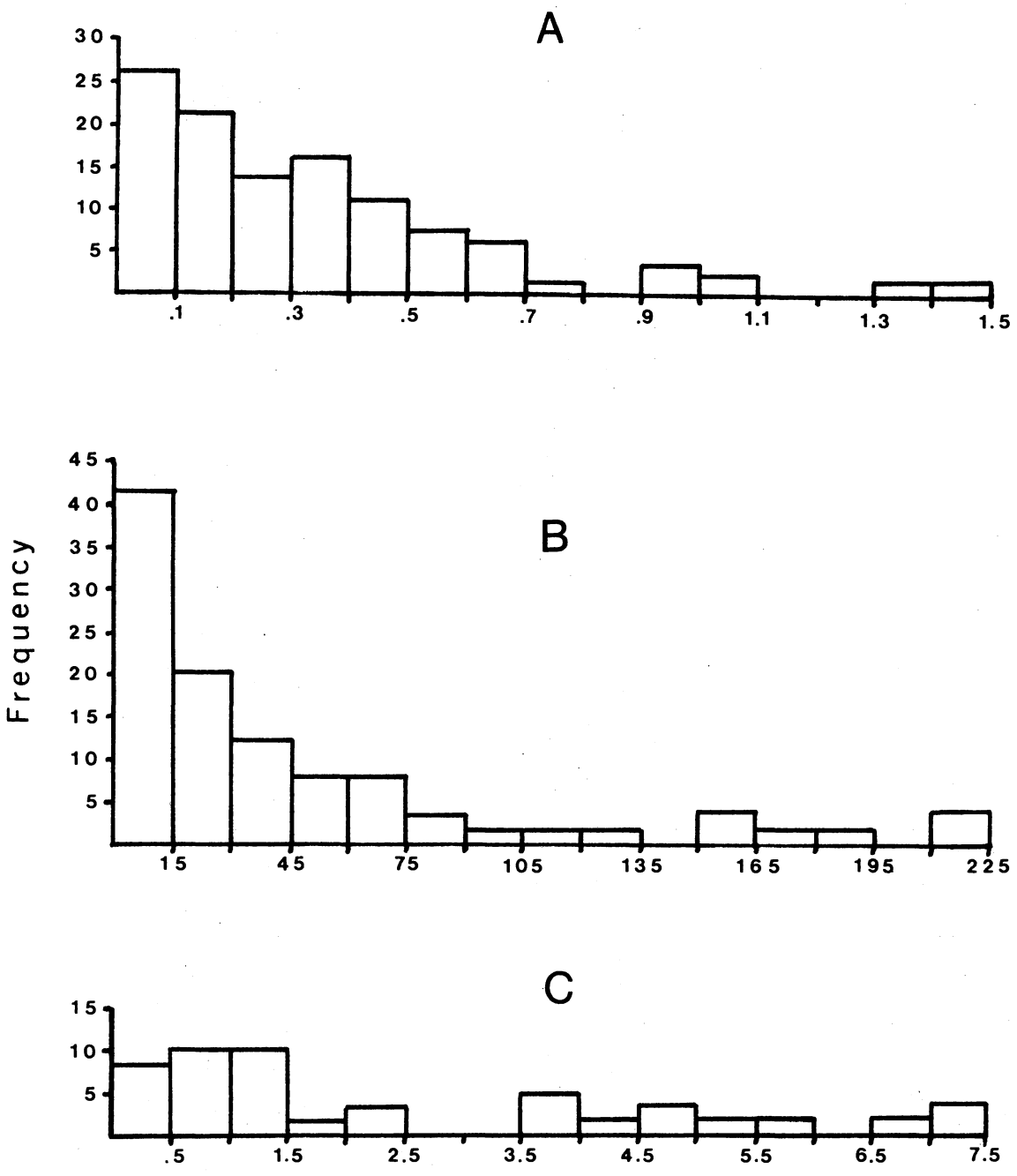

Fig. 18.-Histograms showing the frequency distribution of A) copper in percents, B) molybdenum in parts per million, and C) silver in parts per million.

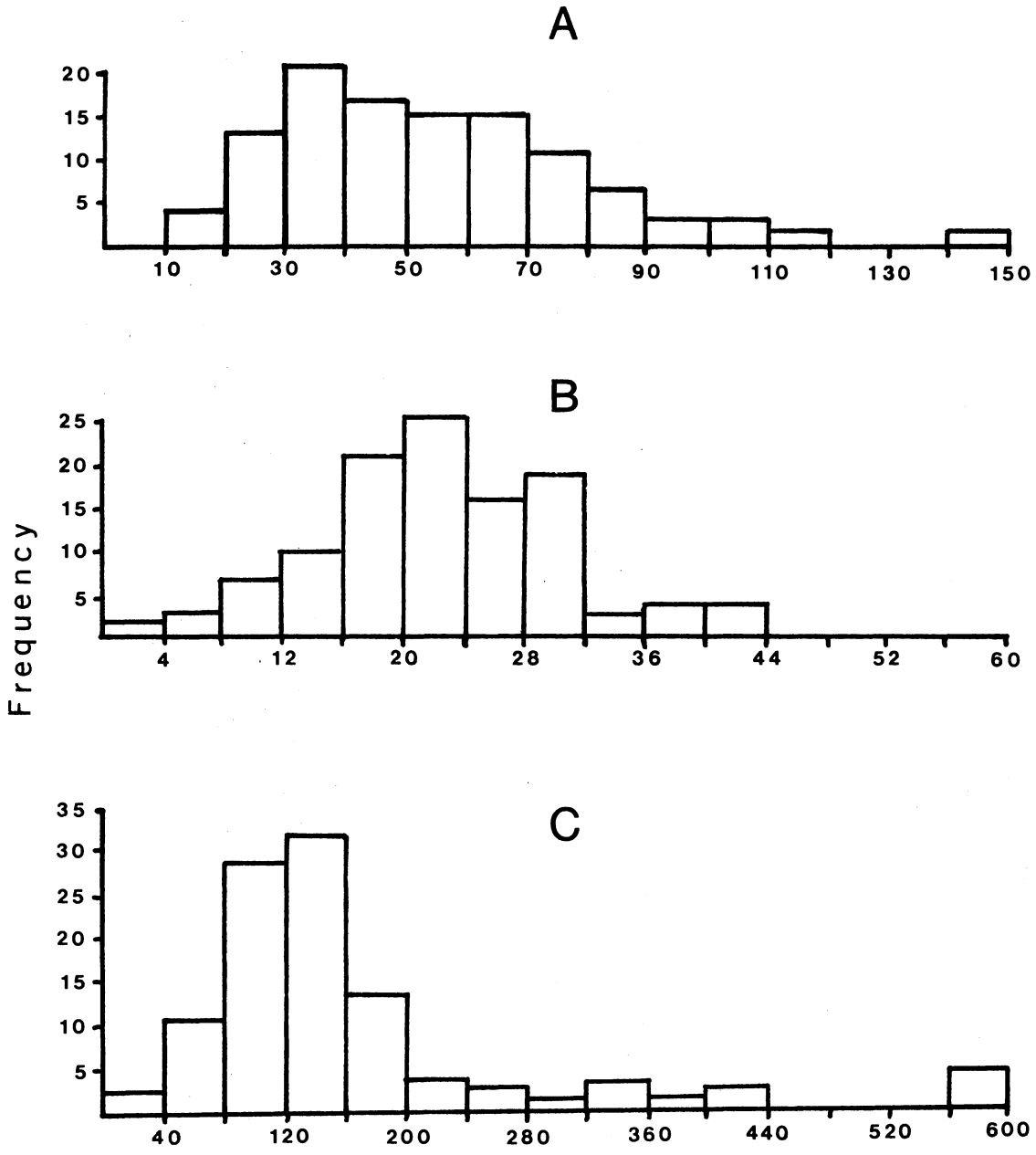

Fig. 19.-Histograms showing the frequency distribution of A) zinc, B) lead, and C) manganese, all in parts per million.

for molybdenum in porphyry copper deposits. The average value of molybdenum determined in this study of the Copper Cities deposit is .0065 percent. Molybdenum is concentrated in the minus 80-mesh fraction of analyzed samples (Table III).

The distribution of molybdenum is similar to that of copper and sericite (Figs. 10, 11, 12). The highest molybdenum concentrations occur along the granite porphyry-quartz monzonite contact. The mineralization tends to decrease with depth as does copper and sericite. The only variation in molybdenum distribution is at the southern end of the 3645 foot level, in the proximity of the Coronado fault zone (Fig. 10). This deviation is a result of differences in the mobility of molybdenum and copper under supergene conditions due to the percolation of oxidizing water downward through the fault zone.

Zinc

The average value of zinc is 54 ppm in the deposit. The plus 80-mesh fraction ratios listed in Table III indicate that zinc concentration is relatively high in the coarse fraction. This can be attributed to the substitution of Zn^{+2} for Fe^{+2} in the structure of biotite. Both Zn^{+2} and Fe^{+2} have an ionic radius of .74Å.

The distribution of zinc, shown in Figures 10, 11, and 12, coincides with copper and sericite distribution and diminishes with depth.

Silver

Silver values associated with the deposit average 2.2 ppm. The background value for silver in U.S.G.S. standard GSP-1 (granodiorite) is .07 ppm (Table I), therefore, all analyzed samples with detectable

silver concentrations were considered to be anomalous. Silver, like copper and molybdenum, is concentrated in the minus 80-mesh fraction of the samples (Table III).

Silver distribution is nearly identical to that of zinc in the deposit (Figs. 10, 11, 12). The silver coincides with maximum sericitic alteration and diminishes in concentration with depth. In a summary of major and minor metal distribution in porphyry copper deposits, Jerome (1966) categorizes silver as occurring both in the central zone with copper, molybdenum, and gold, and to a lesser extent in the fringe zone with lead and zinc.

Manganese

The average value of manganese in the deposit is 180 ppm. The minus 80 versus plus 80-mesh fraction ratio of manganese indicates that the metal is more concentrated in the minus 80-mesh fraction (Table III).

For the most part, manganese distribution correlates with that of the other trace elements in the ore body (Figs. 11, 12). Figure 10, however, shows that the distribution of manganese varies considerably from that of the other trace elements. Wide zones of manganese occur near the Coronado and Drummond fault zones (refer to Fig. 5). These fault zones were responsible for channeling oxidizing waters downward, which altered manganese-rich minerals and concentrated the metal as an oxide.

Lead

The lead content of the ore body averages 22 ppm. Lead has the

highest percentage concentration in the plus 80-mesh fraction of the crushed samples (Table III). This lead concentration is associated with the potassium feldspar. Shrivastava and Proctor (1962) concluded that the lead content (16-25 ppm) of the Searchlight quartz monzonite in Nevada may be attributed to the feldspars.

Substitution for potassium in the silicate structure would be the most likely location of lead in the feldspar. Pb^{+2} has an ionic radius of 1.32Å while K^{+} is 1.33Å. Substitution is facilitated by the equalizing of electrovalent charges as in the following formula:

$$KAlSi_3O_8 + Pb^{+2} + Al^{+3} \rightarrow PbAl_2Si_2O_8 + K^{+} + Si^{+4}$$

This is a thermodynamically stable structure with the geometry of orthoclase (Slawson and Nackowski, 1959). Slawson and Nackowski further determined that porphyry copper deposits with related lead mineralization characteristically have high trace lead values in the potash feldspars, while deposits with sparse lead mineralization have correspondingly low trace lead values in the K-feldspars. They found that 25 ppm and above was the cut-off value for lead-producing deposits. The 22 ppm lead value for the Copper Cities deposit thus reflects the lack of economic lead mineralization in the mine.

Distribution of maximum lead values coincides with the distribution of the other trace elements in the ore body (Figs. 10, 11, 12). High lead values are also associated with the zone of maximum sericitic alteration.

CHAPTER VI

CONCLUSIONS

1) The Copper Cities deposit contains four hydrothermal alteration zones. The potassic zone, defined by the formation of secondary potassium feldspar and biotite, occurs in a deep core below the ore body. The phyllic zone, represented by maximum sericitic alteration, forms a central halo surrounding the potassic core and contains the ore body. The third zone, intermediate argillic alteration, is characterized by montmorillonite and kaolinite. This alteration grades inward into the phyllic zone. Propylitic alteration, delineated by previous workers, is the limit of extensive hydrothermal alteration on the borders of the deposit.

2) Kaolinite of supergene origin occurs beneath the secondary chalcocite zone. The kaolinite is in a blanket-shaped configuration in the zone of intense sericitic alteration. It formed from sericite during the neutralization of acidic fluids responsible for the formation of chalcocite. The kaolinite is a product of supergene activity initiated during the present erosional cycle. It effectively separates the zone of secondary enrichment from the protore and indicates that the bottom limit of enrichment has been reached.

3) Copper in the funnel-shaped ore body averages .35 percent. The trend of copper distribution at depth indicates a possible extension of the ore body to the southwest. Molybdenum values averaged .0065

percent. The molybdenum coincides with copper distribution and is concentrated along the granite porphyry-quartz monzonite contact. The silver content of the deposit averaged 2.2 ppm. The distribution of silver also conforms to that of copper and molybdenum. Copper, molybdenum, and silver coincide with phyllic alteration.

Lead, zinc, and manganese are present in normal background concentrations in the deposit. Lead is localized in the potassium feldspar as an ionic substitute for potassium. Zinc is associated with biotite as a probable substitute for iron.

REFERENCES CITED

Anderson, C. A., 1950, Alteration and metallization in the Bagdad porphyry copper deposit, Arizona: Econ. Geol., v. 45, p. 609-625.

_____, 1968, Arizona and adjacent New Mexico, in Ridge, J. D., ed., Ore Deposits in the United States 1933-1967 (Graton-Sales vs. 1 & 2): New York, A.I.M.E., p. 1162-1190.

Brown, G., 1961, The X-ray identification and crystal structure of clay minerals: Mineralog. Soc. of London, 2nd ed., 544 p.

Burnham, C. W., 1962, Facies and types of hydrothermal alteration: Econ. Geol., v. 57, p. 768-784.

Carroll, D., 1970, Clay minerals: a guide to their X-ray identification: Geol. Soc. America Special Paper 126, 80 p.

Creasy, S. C., 1966, Hydrothermal alteration, in Titley, S. R., and Hicks, C. L., eds., Geology of the Porphyry Copper Deposits, Southwestern North America: Tucson, Arizona, The University of Arizona Press, p. 51-74.

Flanagan, F. J., 1969, U. S. Geological Survey standards - II, first compilation of data for the new U.S.G.S. rocks: Geochim. et Cosmochim. Acta, v. 33, p. 81-120.

Guilbert, J. M., and Lowell, J. D., 1974, Variations in zoning patterns in porphyry ore deposits: Canadian Mining Metall. Bull., v. 67, p. 99-109.

Hemley, J. J., and Jones, W. R., 1964, Chemical aspects of hydrothermal alteration with emphasis on hydrogen metasomatism: Econ. Geol., v. 59, p. 538-569.

Jerome, S. E., 1966, Some features pertinent in exploration of porphyry copper deposits, in Titley, S. R., and Hicks, C. L., eds., Geology of the Porphyry Copper Deposits, Southwestern North America: Tucson, Arizona, The University of Arizona Press, p. 75-86.

Krauskopf, K. B., 1967, Introduction to geochemistry: New York, McGraw-Hill Book Co., 721 p.

Lowell, J. D., and Guilbert, J. M., 1970, Lateral and vertical alteration-mineralization zoning in porphyry ore deposits: Econ. Geol., v. 65, p. 373-408.

Meyer, C., and Hemley, J. J., 1967, Wall rock alteration, in Barnes, H. L., ed., Geochemistry of Hydrothermal Ore Deposits: New York, Holt, Rinehart and Winston, p. 166-235.

Meyer, C., Shea, E. P., Goddard, C. C., et al., 1968, Ore deposits at Butte, Montana, in Ridge, J. D., ed., Ore Deposits in the United States 1933-1967 (Graton-Sales vs. 1 & 2): New York, A.I.M.E., p. 1373-1416.

Peterson, N. P., Gilbert, C. M., and Quick, G. L., 1946, Hydrothermal alteration in the Castle Dome copper deposit, Arizona: Econ. Geol., v. 41, p. 820-840.

_____, 1954, Copper Cities copper deposit, Globe-Miami district, Arizona: Econ. Geol., v. 49, p. 362-377.

_____, 1962, Geology and ore deposits, Globe-Miami district, Arizona: U. S. Geol. Surv. Prof. Paper 342, 151 p.

Ransome, F. L., 1903, Geology of the Globe copper district, Arizona: U. S. Geol. Surv. Prof. Paper 12, 168 p.

_____, 1919, The copper deposits of Ray and Miami, Arizona: U. S. Geol. Surv. Prof. Paper 115, 192 p.

Rose, A. W., and Baltosser, W. W., 1966, The porphyry copper deposits at Santa Rita, New Mexico, in Titley, S. R., and Hicks, C. L., eds., Geology of the Porphyry Copper Deposits, Southwestern North America: Tucson, Arizona, The University of Arizona Press, p. 205-220.

Shepard, S. M. F., Nielsen, R. L., and Taylor, H. P., Jr., 1969, Oxygen and hydrogen isotope ratios of clay minerals from porphyry copper deposits: Econ. Geol., v. 64, p. 755-777.

Shrivastava, J. N., and Proctor, P. D., 1962, Trace element distribution in the Searchlight, Nevada quartz monzonite stock: Econ. Geol., v. 57, p. 1062-1070.

Simmons, W. W., and Fowells, J. E., 1966, Geology of the Copper Cities mine, in Titley, S. R., and Hicks, C. L., eds., Geology of the Porphyry Copper Deposits, Southwestern North America: Tucson, Arizona, The University of Arizona Press, p. 151-156.

Slawson, W. F., and Nackowski, M. P., 1959, Trace lead in potash feldspars associated with ore deposits: Econ. Geol., v. 54, p. 1543-1555.

Still, A. R., 1962, Uranium at Copper Cities and other porphyry copper deposits, Miami district, Arizona: unpub. Ph.D. thesis, Harvard Univ., Cambridge, Mass., 108 p.

Weaver, C. E., and Pollard, L. D., 1973, The chemistry of clay minerals: New York, Elsevier Scientific Publishing Co., 213 p.

APPENDIX

TRACE ELEMENT ANALYSES, CLAY MINERAL ANALYSES

TABLE IV

TRACE ELEMENT ANALYSES

Sample[1] No.	Cu (percent)	Mo (ppm)	Zn (ppm)	Ag[2] (ppm)
DDH - 500				
3645	.20	59	25	.6
3550	.32	27	57	-
3460	.50	27	65	1.4
3380	.45	20	59	-
3340	.09	26	50	.5
DDH - 501				
3645	.07	7	32	.5
3550	.19	15	75	-
3460	.27	9	60	1.1
3380	.33	20	36	-
3340	.62	6	48	8.0
DDH - 502				
3460	.18	846	34	.8
3380	.52	152	56	8.1
3340	.31	106	42	1.3
DDH - 503				
3735	.01	30	33	.6
3645	.03	2	38	.2
3550	.09	47	27	.4
3460	.18	7	34	.8
3380	.06	7	26	.2
3340	.06	8	23	.2
3340A[3]	.02	4	12	.1
DDH - 505				
3735	.21	7	72	-
3645	.04	3	30	.3
3550	.35	5	60	-
3460	.31	15	63	2.0
3380	.09	5	49	-
3340	.39	7	92	.8

TABLE IV (Continued)

Sample[1] No.	Cu (percent)	Mo (ppm)	Zn (ppm)	Ag[2] (ppm)
DDH - 506				
3735	.07	8	23	-
3645	.34	327	54	1.4
3550	.12	7	37	-
3460	.65	35	58	4.4
3380	.52	22	58	-
3340	.45	367	40	1.1
DDH - 510				
3735	.02	9	35	-
3645	.65	8	53	1.7
3550	.04	6	12	-
3460	.13	8	42	1.0
3420	.05	7	53	-
DDH - 314				
3735	.90	133	17	3.9
3645	1.50	42	14	2.2
3550	.61	48	19	1.2
3460	.31	77	19	.8
3380	.29	214	24	.8
3340	.23	34	35	1.2
3340A[3]	.07	17	17	.4
DDH - 317				
3735	.90	212	17	-
3645	.53	65	10	1.4
3550	.57	77	20	3.7
3460	.39	162	18	2.0
DDH - 333				
3735	1.09	66	20	-
3645	.47	60	19	1.2
3550	.53	62	17	8.3
3460	.75	104	17	4.8
3380	.30	66	17	.9
3340	.17	39	16	.4

TABLE IV (Continued)

Sample[4] No.	Cu (percent)	Mo (ppm)	Zn (ppm)	Ag[2] (ppm)
3735 level				
PS - 36	.24	65	49	-
PS - 37	.21	7	70	-
PS - 38	.43	53	54	-
PS - 39	.47	192	93	4.7
PS - 40	.11	37	32	-
PS - 40A[3]	.02	6	17	-
PS - 41	.59	33	62	-
PS - 42	.67	67	38	3.7
PS - 42A[3]	.13	6	21	-
PS - 43	.03	68	28	-
3645 level				
PS - 21	.17	19	28	-
PS - 22	.39	22	63	-
PS - 23	1.05	316	111	5.9
PS - 30	.16	36	70	-
PS - 31	.06	8	40	-
PS - 32	.46	21	43	-
PS - 32A[3]	.11	0	24	-
PS - 33	.27	12	38	-
PS - 34	.06	58	38	-
PS - 35	.12	22	29	-
PS - 35A[3]	.05	16	24	-
PS - 44	.18	18	37	-
PS - 44A[3]	.04	10	19	-
3550 level				
PS - 17	.27	18	67	-
PS - 17A[3]	.11	5	47	-
PS - 18	.25	28	94	-
PS - 19	.45	48	87	-
PS - 19A[3]	.10	22	34	-
PS - 20	.09	5	31	-
PS - 24	.09	167	27	-
PS - 25	.96	405	89	-
PS - 26	.24	27	49	-
PS - 27	.69	154	61	6.5
PS - 28	.49	7	58	-
PS - 29	.31	6	47	-

TABLE IV (Continued)

Sample[4] No.	Cu (percent)	Mo (ppm)	Zn (ppm)	Ag[2] (ppm)
3460 level				
PS - 8	.14	6	44	-
PS - 9	.08	60	101	-
PS - 10	.54	33	53	3.8
PS - 11	.30	6	144	-
PS - 12	.48	8	71	-
PS - 13	.31	36	64	-
PS - 14	.14	6	84	-
PS - 15	.11	18	31	-
PS - 16	.15	3	33	-
3380 level				
PS - 1	.18	228	35	-
PS - 2	1.37	7	108	16.3
PS - 3	.12	8	63	-
PS - 4	.25	51	39	-
PS - 5	.42	33	78	-
PS - 6	.31	13	67	-
PS - 7	.45	6	51	-
3340 level				
PS - 74	.67	38	60	5.1
PS - 75	.10	12	30	-
PS - 76	.17	6	35	-

[1]DDH denotes dimaond drill hole sample.

[2](-) sample not analyzed.

[3]+80 mesh fraction of sample.

[4]PS-pit wall samples listed according to bench elevations.

TABLE IV (Continued)

Sample[1] No.	Pb (ppm)	Mn (ppm)
DDH - 500		
3645	9	77
3550	41	193
3460	24	159
3380	25	135
3340	27	177
DDH - 501		
3645	37	116
3550	25	143
3460	24	145
3380	30	176
3340	15	98
DDH - 502		
3460	8	258
3380	23	101
3340	20	111
DDH - 503		
3735	4	43
3645	15	122
3550	10	97
3460	12	129
3380	31	150
3340	21	74
3340A[2]	20	25
DDH - 505		
3735	6	638
3645	28	57
3550	25	149
3460	30	224
3380	28	188
3340	28	620

TABLE IV (Continued)

Sample No.[1]	Pb (ppm)	Mn (ppm)
DDH - 506		
3735	15	136
3645	15	129
3550	30	161
3460	13	101
3380	20	184
3340	36	86
DDH - 510		
3735	23	122
3645	9	582
3550	1	49
3460	20	128
3420	30	150
DDH - 314		
3735	17	134
3645	14	88
3550	19	179
3460	19	153
3380	24	122
3340	35	141
3340A[2]	17	79
DDH - 317		
3735	17	125
3645	10	182
3550	20	351
3460	18	302
DDH - 333		
3735	20	97
3645	19	201
3550	17	339
3460	17	197
3380	17	191
3340	16	147

TABLE IV (Continued)

Sample[3] No.	Pb (ppm)	Mn (ppm)
3735 level		
PS - 36	27	110
PS - 37	30	242
PS - 38	12	145
PS - 39	23	853
PS - 40	20	65
PS - 40A[2]	17	28
PS - 41	30	353
PS - 42	22	106
PS - 42A[2]	22	43
PS - 43	22	112
3645 level		
PS - 21	33	48
PS - 22	22	406
PS - 23	17	143
PS - 30	29	259
PS - 31	28	123
PS - 32	16	146
PS - 32A[2]	10	43
PS - 33	30	120
PS - 34	24	98
PS - 35	25	109
PS - 35A[2]	25	92
PS - 44	24	117
PS - 44A[2]	19	88
3550 level		
PS - 17	42	151
PS - 17A[2]	25	117
PS - 18	18	320
PS - 19	16	609
PS - 19A[2]	11	171
PS - 20	20	106
PS - 24	28	107
PS - 25	21	145
PS - 26	37	119
PS - 27	22	179
PS - 28	20	120
PS - 29	17	163

TABLE IV (Continued)

Sample[3] No.	Pb (ppm)	Mn (ppm)
3460 level		
PS - 8	28	109
PS - 9	18	202
PS - 10	30	109
PS - 11	24	596
PS - 12	28	137
PS - 13	22	150
PS - 14	40	401
PS - 15	25	107
PS - 16	30	85
3380 level		
PS - 1	16	72
PS - 2	30	652
PS - 3	22	206
PS - 4	15	97
PS - 5	13	159
PS - 6	19	186
PS - 7	26	109
3340 level		
PS - 74	22	133
PS - 75	21	154
PS - 76	22	82

[1]DDH denotes diamond drill hole sample.

[2]+80 mesh fraction of sample.

[3]PS - pit wall samples listed according to bench elevations.

TABLE V

CLAY MINERAL ANALYSES[1]

Sample[2] No.	Sericite (percent)	Montmorillonite (percent)	Kaolinite (percent)
DDH - 500			
3645	86	0	14
3550	24	56	20
3460	64	23	13
3380	22	71	7
3340	79	6	15
DDH - 501			
3645	63	18	19
3550	20	67	13
3460	24	61	15
3380	27	68	8
3340	90	0	10
DDH - 502			
3460	91	0	9
3380	79	11	10
3340	68	25	7
DDH - 503			
3735	100	0	0
3645	81	0	19
3550	100	0	0
3460	100	0	0
3380	70	16	14
3340	37	43	20
3340A[3]	-	-	-
DDH - 505			
3735	57	14	29
3645	54	4	42
3550	55	30	15
3460	34	50	16
3380	73	0	27
3340	40	41	19

TABLE V (Continued)

Sample[2] No.	Sericite (percent)	Montmorillonite (percent)	Kaolinite (percent)
DDH - 506			
3735	82	9	9
3645	77	11	12
3550	20	68	12
3460	73	27	0
3380	51	32	17
3340	60	32	8
DDH - 510			
3735	39	30	31
3645	57	34	9
3550	84	0	16
3460	39	33	28
3420	35	38	27
DDH - 314			
3735	78	10	12
3645	77	9	14
3550	43	40	17
3460	20	63	17
3380	58	23	19
3340	62	19	19
3340A[3]	-	-	-
DDH - 317			
3735	88	0	12
3645	70	0	30
3550	23	61	16
3460	5	90	5
DDH - 333			
3735	47	49	4
3645	69	12	19
3550	70	0	30
3460	72	13	15
3380	16	72	12
3340	70	15	15

TABLE V (Continued)

Sample[4] No.	Sericite (percent)	Montmorillonite (percent)	Kaolinite (percent)
3735 level			
PS - 36	91	0	9
PS - 37	77	15	8
PS - 38	63	22	15
PS - 39	83	2	15
PS - 40	98	2	0
PS - 40A[3]	-	-	-
PS - 41	76	0	24
PS - 42	83	11	6
PS - 42A[3]	-	-	-
PS - 43	68	14	18
3645 level			
PS - 21	58	28	14
PS - 22	69	0	31
PS - 23	100	0	0
PS - 30	50	19	31
PS - 31	31	49	20
PS - 32	67	20	13
PS - 32A[3]	-	-	-
PS - 33	72	12	16
PS - 34	16	72	12
PS - 35	32	40	28
PS - 35A[3]	-	-	-
PS - 44	31	46	23
PS - 44A[3]	-	-	-
3550 level			
PS - 17	59	23	18
PS - 17A[3]	-	-	-
PS - 18	62	29	9
PS - 19	100	0	0
PS - 19A[3]	-	-	-
PS - 20	29	48	23
PS - 24	37	52	11
PS - 25	44	42	14
PS - 26	44	46	10
PS - 27	63	10	27
PS - 28	81	19	0
PS - 29	51	27	22

TABLE V (Continued)

Sample[4] No.	Sericite (percent)	Montmorillonite (percent)	Kaolinite (percent)
3460 level			
PS - 8	29	46	25
PS - 9	94	0	6
PS - 10	100	0	0
PS - 11	67	27	6
PS - 12	58	35	7
PS - 13	57	37	6
PS - 14	25	47	28
PS - 15	27	50	23
PS - 16	32	52	16
3380 level			
PS - 1	14	75	11
PS - 2	29	61	10
PS - 3	27	55	18
PS - 4	42	47	11
PS - 5	36	60	4
PS - 6	28	58	14
PS - 7	21	70	9
3340 level			
PS - 74	50	41	9
PS - 75	39	52	9
PS - 76	45	40	15

[1]Clay percentages calculated from total clay content of rock sample.

[2]DDH denotes diamond drill hole sample.

[3]80 mesh fraction of sample (no clay content).

[4]PS - pit wall samples listed according to bench elevations.

VITA 2

Thomas Willis Reed

Candidate for the Degree of

Master of Science

Thesis: TRACE ELEMENT DISTRIBUTION AND ALTERATION STUDY OF THE COPPER CITIES DEPOSIT, ARIZONA

Major Field: Geology

Biographical:

Personal Data: Born in Bartlesville, Oklahoma, October 3, 1951, the son of Mr. and Mrs. Thomas Morse Reed.

Education: Graduated from College High School, Bartlesville, Oklahoma, in May, 1969; received the Bachelor of Science degree from Oklahoma State University, Stillwater, Oklahoma, in May, 1973, with a major in Geology; completed the requirements for the Master of Science degree from Oklahoma State University in July, 1975, with a major in Geology.

Professional Experience: Graduate field assistant, Oklahoma Geology Camp, Canon City, Colorado, summer, 1974; Graduate research assistant, Department of Geology, Oklahoma State University, 1974-1975. Student member of the American Institute of Mining, Metallurgical, and Petroleum Engineers.

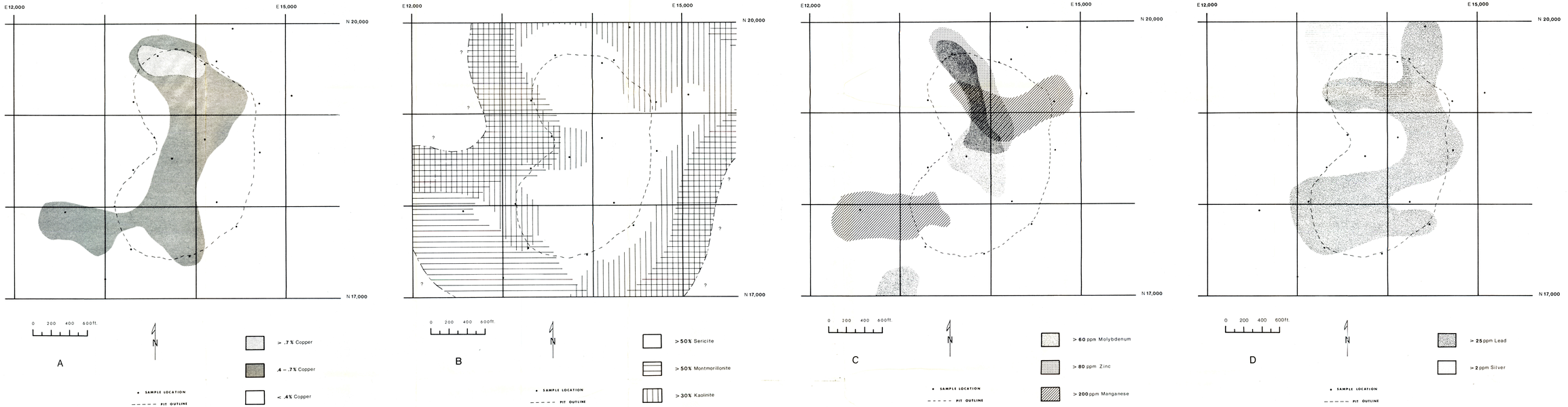

FIGURE 10

DISTRIBUTION OF COPPER (A), CLAY MINERALS (B), MOLYBDENUM, ZINC, MANGANESE (C), AND LEAD, SILVER (D) ON THE 3645 FOOT LEVEL OF THE COPPER CITIES DEPOSIT, ARIZONA

THOMAS W. REED 1975

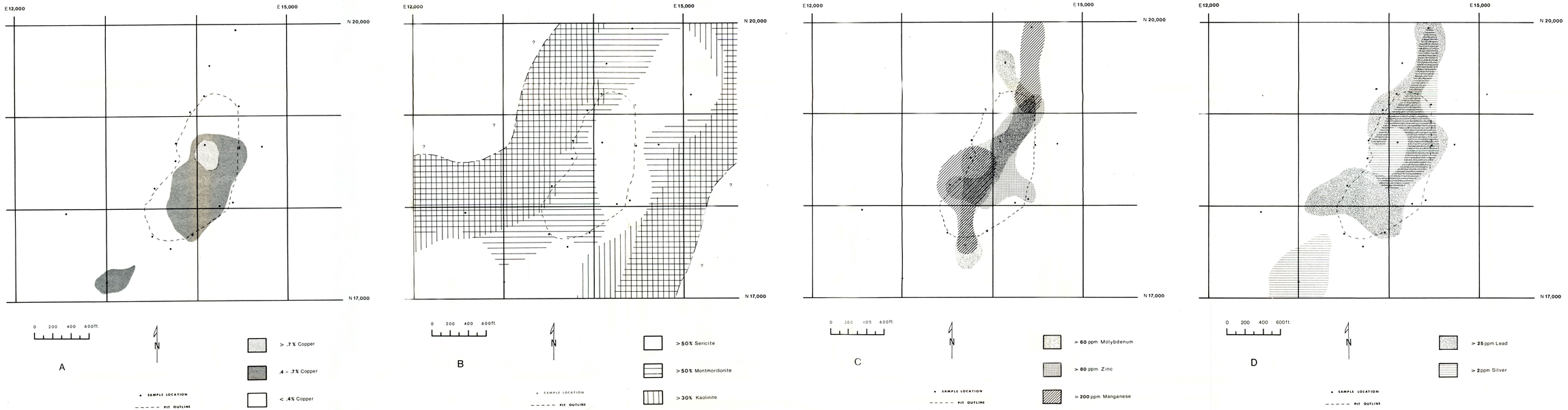

FIGURE 11

DISTRIBUTION OF COPPER (A), CLAY MINERALS (B), MOLYBDENUM, ZINC, MANGANESE (C), AND LEAD, SILVER (D) ON THE 3460 FOOT LEVEL OF THE COPPER CITIES DEPOSIT, ARIZONA

THOMAS W. REED 1975

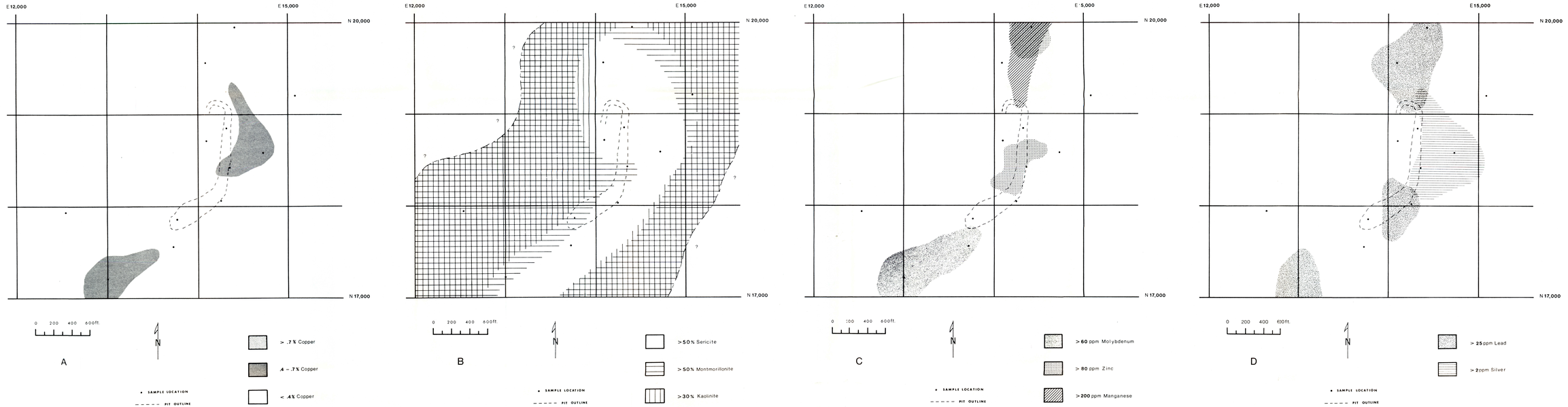

FIGURE 12

DISTRIBUTION OF COPPER (A), CLAY MINERALS (B), MOLYBDENUM, ZINC, MANGANESE (C), AND LEAD, SILVER (D) ON THE 3340 FOOT LEVEL OF THE COPPER CITIES DEPOSIT, ARIZONA

THOMAS W. REED 1975